Master's thesis

NTNU
Norwegian University of Science and Technology
Faculty of Engineering
Department of Energy and Process Engineering

Christian Mellbye and Sondre Bekken

Utilizing LNG for low temperature freezing system for tuna

Master's thesis in Mechanical engineering
Supervisor: Trygve M. Eikevik
June 2020

NTNU
Norwegian University of
Science and Technology

Christian Mellbye and Sondre Bekken

Utilizing LNG for low temperature freezing system for tuna

Master's thesis in Mechanical engineering
Supervisor: Trygve M. Eikevik
June 2020

Norwegian University of Science and Technology
Faculty of Engineering
Department of Energy and Process Engineering

NTNU
Norwegian University of
Science and Technology

Summary

In this thesis, proposals of low-temperature freezer designs using liquid natural gas (LNG) as a cold sink has been investigated. The freezer temperature can reach -90°C with the purpose of freezing tuna fish.

Tuna fish is a highly valuable food product, especially in the open markets of Japan. However, correct processing of the tuna is essential to preserve the quality and, consequently - the value. To maintain this quality, low-temperature freezers are critical infrastructure. As of today, there exist no such freezers in Norway. LNG is stored at a temperature of -162°C. During vaporization, LNG is heated to ambient temperature. Several LNG vaporization terminals are located along the coast of Norway, where also the tuna fish is caught. Utilizing the LNG as a cold sink for the tuna freezer enables opportunities to reach ultra-low temperatures without consuming high quantities of electrical power. Simulations of different tuna fish sizes and freezer designs were performed to find the best proposal for a freezer design.

Thermophysical properties of the tuna fish are used in a model to investigate the freezing time and the freezing effect. The model is written in MATLAB and calculates how the temperature distribution inside the tuna develops with time. Due to the lack of empirical data such as the thermophysical properties of the tuna at low temperatures, some assumptions were made.

Furthermore, an insulated container, was chosen as the freezing facility due to the low price and easy mobility. The container consists of a fan and a heat exchanger connected to the LNG flow. The fan circulates the air over the tunas, and the heat exchanger assures that the freezer temperature is kept to the desired level. Investigations of how the freezer operates were solved in Dymola, a software that is beneficial to solve transient processes. Results from the tuna model were integrated into the simulation to describe the heat load of the freezer. Operational conditions of the freezer, such as power consumption and LNG mass flow, were acquired by the simulation results.

Sammendrag

I denne masteroppgaven er det blitt undersøkt muligheter for å bruke flytende naturgass (LNG) som en kuldekilde til en lav-temperatur fryser. Fryseren kan nå temperaturer på -90 °C med formålet å fryse tunfisk.
Tunfisk er et svært verdifullt matprodukt, spesielt på markedene i Japan. Riktig prosessering av tunfisk er imidlertid viktig for å bevare kvaliteten og dens verdi. Det er kritisk med lavtemperaturfrysere for å opprettholde kvaliteten på tunfisken. Per i dag eksisterer det ingen slike frysere i Norge. LNG lagres ved en temperatur på -162 °C. Under fordamping blir LNG oppvarmet til omgivelsestemperatur. Flere LNG-fordampingsterminaler ligger langs kysten av Norge, hvor også tunfisk blir fanget. Ved å bruke LNG som en kuldekilde til fryseren er det mulig å oppnå ultra-lave temperaturer uten å bruke store mengder strøm. Simuleringer av forskjellige tunfiskstørrelser med forskjellig fryserdesign har blitt utført for å finne det beste forslaget til en lavtemperaturfryser for tunfisk.

De termofysiske egenskapene til tunfisken ble brukt for å undersøke frysetiden og varmeeffekten. Modellen er skrevet i programmet MATLAB og den beregner hvordan temperaturfordelingen inne i tunfisken utvikler seg med tiden. På grunn av mangel på empiriske data som termofysiske egenskaper til tunfisken ved lave temperaturer, ble det gjort noen antagelser.

Videre ble en isolert containeren valgt som fryseanlegg på grunn av lav kostnad og fleksibel mobilitet. Containeren består av en vifte og en varmeveksler koblet til LNG-anlegget. Viften sirkulerer luften over tunfiskene, og varmeveksleren sikrer at frysetemperaturen holdes til et ønsket temperaturnivå. Undersøkelser av hvordan fryseren fungerer, ble løst i Dymola, en programvare som er fordelaktig for å løse prosesser som forandres ved tiden. Resultatene fra tunfiskmodellen i Matlab ble integrert i simuleringen i Dymola for å finne effekten fryseren hadde behov for. Ved bruk av Dymola og Matlab ble det avgjort hvor mye strømforbruk og massestrøm av LNG som var nødvendig for de ulike løsningene.

Preface

This report is the result of the work with a Master thesis in mechanical engineering at the Department of engineering (IVT) at the Norwegian University of Science and Technology (NTNU) in Trondheim, Norway. The thesis has been developed through the spring semester of 2020.

We would like to thank our supervisor, Trygve Magne Eikevik for guidance and support on writing the thesis. In addition, Ingnat Tolestorebrov played a critical role for guidance and discussion of problems. Furthermore, we thank Marcel Ulrich Ahrens for teaching us Dymola and helped solve the challenges we faced.

We hope that this thesis gives a perspective of the business opportunities utilizing LNG as a cold sink. Also, the thesis provides an understanding of how to process tuna fish to increase the value of the fish. This process technique is not a part of methods carried out today, and we hope this thesis will inspire such methods to be implemented.

Table of Contents

List of Tables

List of Figures

Nomenclature

Roman Symbols

A	Area[m^2]
c	Specific heat capacity [J/kgK]
D	Charateristic dimension [m]
e	effusivity [$J/s^{1/2}m^2K$]
h	Heat Transfer coefficient [W/m^2K]
k	Thermal conductivity [W/mK]
M	Molecular mass [kg/kmol]
m	mass [kg]
P	Pressure [bar]
Q	Heat transfer rate [W]
q	Heat flux density [W/m^2]
R	Universal gas constant [kJ/kgmolK]
T	Temperature [K]
t	Time [s]
V	Volume [m^3]
v	Velocity [m/s]

Greek Symbols

α	Diffusivity [m^2/s]

Δ Difference

∇ Gradient

ρ density [kg/m^3]

θ finite temperature difference [K]

Subscripts

amb Ambient

ci cold fluid inlet

co cold fluid outlet

$evap$ Evaporator

f freezing

hi hot fluid inlet

ho hot fluid outlet

int Initial

s solid

Abbreviations

AAV Ambient air vaporizer

COP Coefficient of performance

$FTCS$ Forward in time, backwards in space

$FTCS$ Forward in time, center in space

GWP Global warming potential

IFV Intermediate fluid vaporizer

IQF Individually quick frozen

LNG Liquid natural gas

$MPET$ Multi port extruded tubes

NG Natural gas

ODP Ozone depletion potential

ORV Open rack vaporizer

PI Proportional Integral

RVP Relative Vapour Pressure

SCV Submerged combustion vaporizer

SIM System information manager

VLE Vapor-liquid equilibrium

Chapter 1

Introduction

Tuna fishing has been illegal in Norway since 1986 due to overfishing and low stocks. International cooperation has led to an increase of stock, and in 2014, Norway was handed out a quota of 31 tons. Since then, the quotas have increased to over 300 tons in 2019 (Fiskeridirektoratet, 2019). Tuna is a highly valuable fish and is especially sought after in Japan. The value of a tuna fish is highly dependent on the quality and how it is processed. Freezing the tuna quickly and to low temperatures is essential to increase the profit.

1.1 Liquid Natural Gas

LNG is natural gas witch is liquefied at a temperature of -162 °C. The reason for liquefying the gas is to increase the density. The liquid require less space per mass so it can be stored and transported in a smaller volume than if it were at gaseous state. At liquid state, the volume is approximately 600 times lower compared to the gas state. When the LNG has reached the destination, the LNG is either stored or regasified. The LNG is heated through a vaporizer to a temperature of approximate 0 °C, enabling the use of the gas. Natural gas (NG) predominately consists of methane (CH_4), with a fraction ranging from 70-90% (Chandra, 2020). The rest is mostly ethane and some small amounts of propane, butane, and nitrogen. The gas is used for industrial, transport, agricultural, and electricity-generating purposes. Most of the natural gas utilized in Norway is used for industrial purposes (68% in 2018) (Statistisksentralbyrå, 2020; Foss and Head, 2007).

1.1.1 Value chain in Norway

Natural gas is found in natural reservoirs below the ground. One example of this is the reservoir Snøhvit, located in Finnmark, Norway. Gas is extracted from the reservoir via an offshore oil rig and transported, via pipes, to a land-based plant called Hammerfest LNG. Since Hammerfest LNG is located far north in Norway, it is not economically beneficial to install a pipe to transport the gas, as this pipe would be long and the investment costs high. However, there is another way of transporting gas. At Hammerfest LNG, the gas is processed before the temperature is lowered to -162°C, condensing the gas into a liquid (liquid natural gas - LNG). Large amounts of LNG could be transported by special ships or trailers.

Figure 1.1: Map of the value chain for NG (green arrow) and LNG (blue arrow) transportation in Norway. The arrows are not accurate destinations, but display the concept of transportation.

The liquid natural gas is transported from Hammerfest to an LNG terminal, where the LNG is heated to a temperature of approximately 0 °C. The heating of the LNG is called the gasification process. Seawater or ambient air is often used as a heat source in the gasification process. The freezing potential is therefore let into the ambient and is not used for purposes as air-condition, district cooling, or food freezing. The low temperature

of the LNG can be useful to food freezing. Since there exists a lot of fishing industry along the coast of Norway as well as 25 LNG terminals (Woll and Svendgård, 2015), it is feasable to combine the gasification process of LNG to fish freezing. There are six companies delivering and handling LNG in Norway. Three of the largest LNG terminals owned by Gasnor is an LNG terminal in Mosjøen, Sunndalsøra, and Lista with 20-30.000 ton, 7-15.000 ton, and 4-10.000 ton, of LNG, delivered each year, respectively. The data was collected from Gasnor.

1.2 Tuna fish quality versus price

The value of a tuna fish is highly dependent of the quality. Fish markets in Japan consume 90% of blue finned tuna (Ottolenghi, 2008a). An article from the department of environmental and natural resource economics states that America stands for 15% of the import of blue finned tuna in Japan (Ottolenghi, 2008b). Marked officials in Japan, together with brokers in the US, has made a grading system to determine the quality of the tuna fish. The four primary attributes of the quality are freshness, fat content, color, and shape. The article is relevant for fresh tuna fish, but can be applied to frozen tuna fish as well (Carroll et al.). The price can have large varieties depended on the quality, as seen in table 1.2. To rate the quality of the tuna, a wholesaler extracts a thin core of flesh from the fish. From this thin core of flesh, the fat and oil consents, color, and outside appearance, are rated, and the fish gets tagged by the correct rating (Ottolenghi, 2008a).

Measurement	% change in price from lowest grade (E) to highest grade (A)
Freshness	17
Fat content	76
Shape	28
Color	65

Figure 1.2: The table display the difference in price between low and high rated tuna quality

1.2.1 Transportation of tuna

Decreasing the cost of transportation of tuna from Norway to Japan is another method to increase the profit of the tuna fish. The transportation is either done by air or sea. Ziegler et al. (2013), a report from SINTEF, has analyzed the two methods of transportation of salamon and compared them against each other. Even though tuna is a different fish, the results can be used due to the similarities of the products and value chain. The report states that salmon transportation by air to Shanghai from Norway has a 2.9 higher impact of greenhouse gas emissions than by sea. Also, air transportation is more expensive for salmon companies. The only reason to transport salmon by air is to deliver a fresh product. If the conservation method can be improved, the fish can be transported by sea instead of air, and still achieve high-quality fish upon delivery in Shanghai. In comparison to tuna, the transportation route would be to Japan, and conservation methods for tuna fish are of

high importance before and during transport. If a solution can be derived where the tuna is transported by sea to Japan, and still preserve the quality, both transportation costs and greenhouse gas emissions would decrease compared to transportation by air.

1.3 Aims of the study

The objective of this thesis is to design a new freezing system, which utilizes the cold from the vaporization of liquid natural gas. The freezer shall be able to reach ultra-low temperatures of -90 °C or lower. A combination of fisheries and industrial plants collaborating in a symbiosis relationship is going to be investigated. On the one hand, an LNG gasification process requires heat exchange to increase the temperature of LNG from -162°C to approximate 0°C. On the other hand, tuna freezing facilities require heat exchange to decrease the temperature of tuna from approximate -2°C to as low as -80°C. Figure 1.3 display the concept of utilizing LNG for freezing tuna. There are several benefits of utilizing this relationship, but also a few challenges. Technical analysis of different system designs, combined with economic feasibility, will provide possible solutions to the problem.

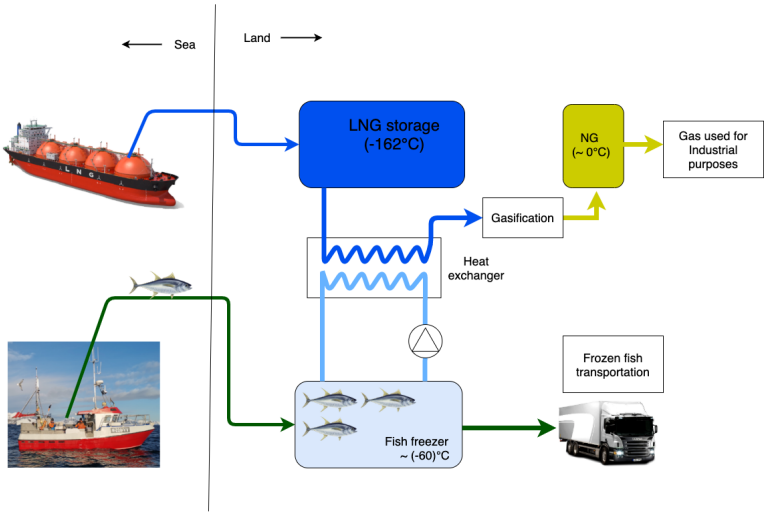

Figure 1.3: Symbiotic relationship between gasification of LNG and fish freezing

Chapter 2

LNG vaporization

To determine the amount of heat capacity the LNG absorbs during vaporization, the mass flow and enthalpy change must be established. Vaporizers manage to increase the temperature of the LNG to ambient temperature, preparing the gas for industrial purposes. The properties of LNG and the existing vaporizer technology will be presented in this chapter.

2.1 Properties of Methane

The gasification of LNG requires substantial amount of heat. To determine the thermophysical properties of LNG is difficult because the composition is not standardized. The properties of methane, NG and LNG can vary by 10% to 20%. Yet, assuming that LNG consist of pure methane provides acceptable indication of empirical analysis of LNG Çengel (2020). Therefore, any calculations referred to as LNG in this thesis is assumed to be methane.

Methane has a boiling point of -161,5°C at atmospheric pressure. Since LNG is stored as saturated liquid, the heat absorbed by the LNG during the gasification process is first latent heat and then sensible heat. The table below shows thermophysical properties at different states of methane.

Methane, P = 1 atm			
Temperature, (°C)	**Density ([kg/m^3])**	**Specific heat (kJ/kg/K)**	**Enthalpy (kJ/kg)**
-161,5 (sat. liquid)	422,4	3,481	-286,5
-165,5 (sat. vapour)	1,816	2,218	224,3
0	0,7177	2,181	568,3

Table 2.1: Properties of methane at 1 atm (Wlodek, 2019).

Latent heat exchange

The latent heat transfer required to vaporize methane from saturated liquid is 510,8 kJ/kg. This vaporization occur at -161,5°C, making it a low temperature freezing potential. Since methane is two-phase during the vaporization, low heat transfer area as well as high heat transfer rates can be reached. Due to these facts, liquid methane (LNG) has high freezing potential when vaporized. On the other hand, problems such as frost formation on the hot side of the heat exchange can occur. This depends on the medium that is used to exchange heat with the LNG.

Sensible heat exchange

When the methane has reached saturated gas state, further heat transfer is required to increase the temperature. The sensible heat transfer required to increase the temperature from -161.5°C to 0 °C is 344 kJ/kg. It is not possible to extract 344 kJ/kg of methane as freezing potential because of the large temperature interval. In addition, large heat transfer area is required to exchange heat of methane gas versus two-phased methane.

2.2 Vaporizing technologies

Vaporization is the transition from the liquid phase to the vapour phase. The vaporizer technology used at a processing terminal is depended on climate, environmental impact, investment cost, site regulations, and available heat source.

2.2.1 Ambient Air Vaporizer

Ambient air vaporizer (AAV) uses ambient air to vaporize the LNG. The design of a typical AAV is a vertical construct consisting of several long and small diameter tubes. The LNG enters the lower part of the pipes, and heat transfer from ambient air occurs. At the top of the pipes, the methane is gaseous and has reached the desired temperature.

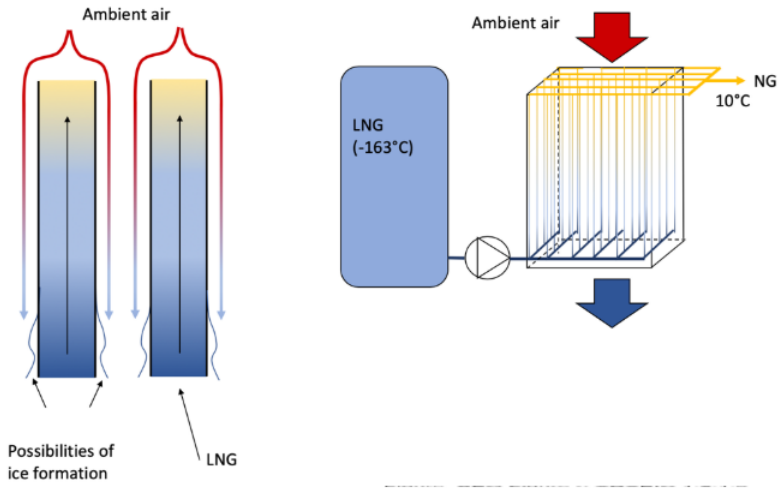

Figure 2.1: Figure shows a Ambient Air Vaporizer system

Figure 2.1 displays the principle of an AAV system; the blue color corresponds to LNG and yellow to NG. The ambient air, which is marked in red color on the figure, passes on the outside of the tubes. The air exchanges heat due to the temperature difference to the LNG.

The airflow can be controlled by either natural or forced convection. Natural convection will occur because of different temperatures in the air (as it is cooled down) and other factors such as wind and pressure differences. Forced convection is applied using fans or other equipment that force the air to pass the tubes. The fan results in increased heat transfer but also increased consumption of electricity.

A challenge to AAV occurs when the ambient air temperature reaches low temperatures (below 0° C). This can take place in certain geographical places, especially during winter. The low ambient temperature affects the heat transfer, and the exit gas will be cooler. As a consequence, the AAV is frequently used in hot climate regions. Another challenge is the formation of ice on the surface of the tubes—the air condensate due to the low surface temperature. Ice formation will continue to grow on the tubes. Ice has a high thermal resistance and will insulate the pipe, hence decrease the heat transfer efficiency. To reduce the ice formation, defrosting has to be implemented in the operation (Gavelli, 2010).

2.2.2 Open Rack Vaporizer

Location is vital to implement the open rack vaporizer (ORV), which is dependent on seawater as a heat source. The preferred seawater temperature for an ORV is above 5° C. The ORV is designed with several tubes mounted vertically beside each other as a panel. LNG is moving inside the tubes from bottom to top, and seawater flows downwards on the external surface of the tubes. The heat transfer is high due to the high heat capacity and density of the seawater. Improved designs such as fins and unique geometry on the tube increase the heat transfer. The material used is typically aluminum alloy that can withstand low temperatures.

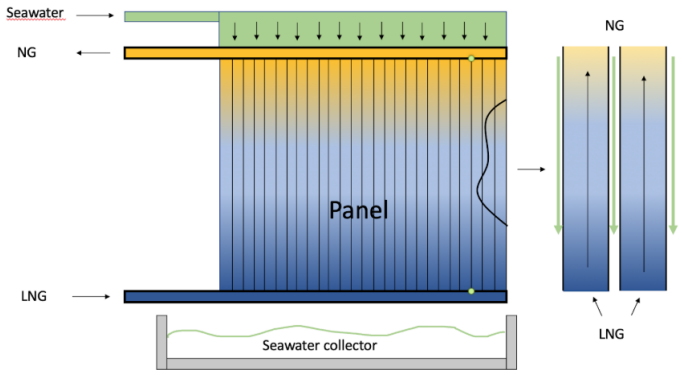

Figure 2.2: The figure shows a Open Rack Vaporizer system.

Figure 2.2 illustrates an ORV. The seawater flows down the panel outside the pipes and the LNG flowing up inside the pipes.

There are multiple challenges related to an ORV system. Since the system uses seawater as heat for the LNG, the development of corrosion is of grave concern. Different methods can be applied to reduce the problem, such as coating the surface or the use of a zinc anode. Also, depending on where the installation is located, seawater can be polluted with sand or other objects that can result in failure for the filters, pumps, or pipes. Filters of different sizes are, therefore, necessary to filtrate and ensure a certain purity of the seawater. Besides, it is necessary to chlorinate the seawater to avoid marine growth in the system (Patel et al., 2013). Furthermore, environmental aspects have to be considered; cold water can damage or reduce biological processes. The correct location of pipes within- and outflow is important to minimize the environmental impact.

Ice formation on the tubes is another challenge to the ORV system. The seawater forms a thick layer of ice on the outside of the tubes due to direct heat transfer between LNG and seawater. The thick ice layer provides high thermal resistance, which then decreases the overall efficiency.

2.2.3 Submerged combustion vaporizer

Submerged Combustion Vaporizer (SCV) vaporize the LNG in tubes that are submerged in a water bath. The water bath has a stable heat source that provides a water temperature

of 10-35 ° C. SCV consumes some natural gas to provide the heat consumption for the water bath. In figure 2.3 a SCV is shown with the water tank, the submerged combustion chamber, and tubes.

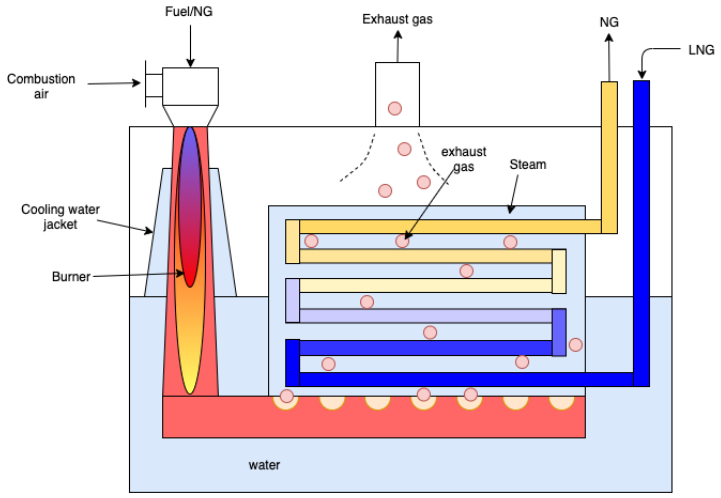

Figure 2.3: The figure shows a Submerged Combustion Vaporizer system

SCV has low investment cost, quick launch, compact structure, and can handle various loads of LNG. The disadvantages of this system are the use of natural gas to gasify LNG. This implies a high-cost operation because a fraction of the LNG will be used in the gasification process and not for industrial purposes. Consumption of NG to heat is quantified in the range of 1% - 2,5% (Patel et al., 2013; Egashira, 2013). Utilizing natural gas causes environmental disadvantages as it ejects greenhouse gases during burning. The water used in the bath is acidic since the combustion gas produces CO_2, which are condensed into the water. Therefore, the water requires a controlled pH value to protect the tubes against corrosion.

2.2.4 Intermediate fluid vaporizer

The Intermediate fluid vaporizer (IFV) is complicated and consists of three main parts; an evaporator, condenser, and a thermometer. Figure 2.4 display the concept of an IFV with a shell-and-tube heat exchanger. The intermediate fluid is held in a close container where it evaporates by heat absorption from seawater. The evaporated gas reaches the tubes where LNG flows and ejects heat resulting in condensation. Due to the intermediate fluid, the IFV avoids ice formation during the vaporization of LNG. Downstream of the condenser, the methane enters a final heat exchanger, filled with seawater, ensuring the desired natural gas temperature.

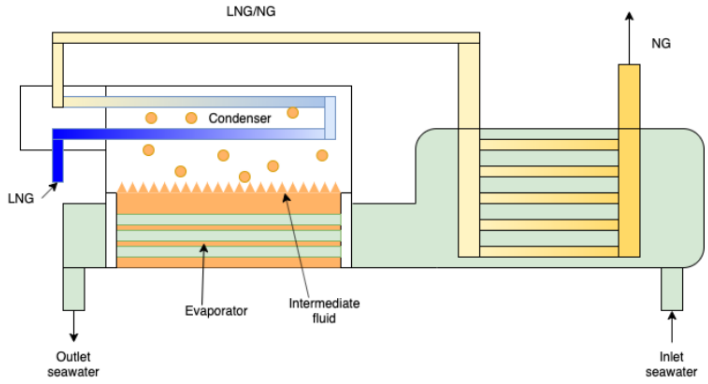

Figure 2.4: The figure shows a Intermediate Fluid Vaporizer system

2.2.5 Comparison of the vaporizers

To decide the correct vaporization technology, several factors have to be taken into account. From an environmental perspective, heat sources such as seawater or ambient air are the most desirable. The utilization of ambient heat sources also depend on the geographical location. Equatorial regions have a higher potential of using the ambient utilities. In table 2.2 a comparison between the different designs are listed.

	AAV	ORV	IFV – seawater as heat source	SCV
Environmental impact	low	Medium (Cold seawater and chloride water)	Medium (Cold seawater and chloride water)	High (NO_x and CO_2 exhaust)
Space requirement and heat transfer area	High	Medium	Medium/low	Low
Geographical location	Warm and dry climate. Also used as peak shave	Cold or warm climates – worse at cold seawater temperatures	Cold or warm climates	Independent of location
Utilities required	Air and electric power	Seawater and electrical power	Seawater and electrical power	Fuel and electrical power
Ice formation	High – frequent defrosting	High – frequent defrosting	Low	Low
Corrosion	Low	High – zinc anode is necessary	High - zinc anode is necessary	Low

Table 2.2: LNG vaporization technology comparison

Chapter 3

Freezing technology

A conventional method of preserving food is to freeze it to temperatures of approximate -24$^{\circ}C$. This can be accomplished by several different methods, depending on the shape and requirements of the food product. Small-sized product has low freezing time and can be frozen on a conveyor belt, whereas large product must be frozen in stable conditions. In this chapter, the main principles of a freezer will be presented along with different freezing technologies.

3.1 Conventional freezing process

The conventional refrigeration system used for freezing fish is often based on a Rankine cycle that consists of one compressor, condenser, expansion valve, and evaporator. The system is referred to as a one-stage cycle and is shown in figure 3.1 with corresponding pressure-enthalpy diagram in figure 3.2. A specific refrigerant cycle in the closed-loop. Figure 3.1 and 3.2 illustrates an ideal cycle.

State 1-2: From state 1, the refrigerant enters the compressor. At state 2, the refrigerant is compressed, and the temperature is at the highest throughout the cycle.

State 2-3: Downstream of state 2, the refrigerant enters the condenser where it rejects heat. Since the condenser is typically located in ambient temperatures, the temperature of the refrigerant between state 2 and 3 has to be higher than the ambient temperature. In figure 3.2, this temperature difference between ambient and the refrigerant is shown as ΔT_c.

State 3-4: At state 3, the refrigerant is saturated liquid. The refrigerant is then expanded, through a valve, to state 4. During this process, both pressure and temperature are lowered.

State 4-1: From state 4, the refrigerant enters the evaporator, which is located in the freezer. In the evaporator, the refrigerant absorbs latent heat at a constant temperature. This evaporation temperature has to be lower than the given freezer temperature, which is usually set to -24°C. This temperature difference between the refrigerant and freezer is shown as ΔT_e in figure 3.2.

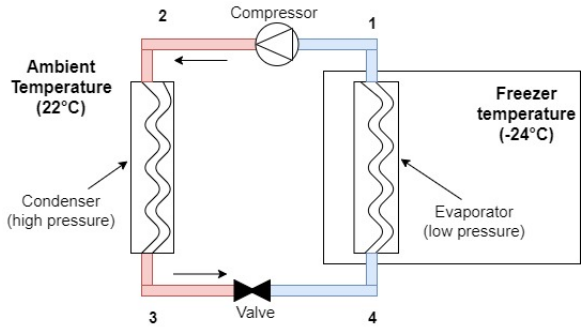

Figure 3.1: The figure shows a single stage compression refrigeration system

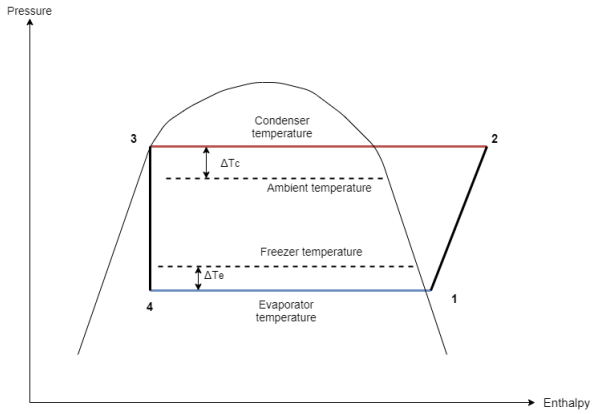

Figure 3.2: A pressure-enthalpy diagram for a single stage compression refrigeration system

There are three main design criteria for a freezer, which must be decided to design the refrigerator (Eikvik, 2020).

1. The required refrigeration capacity

2. The required temperature in the freezer

3. The ambient temperature that the heat shall be rejected to

First, the size of the evaporator and the condenser has to be decided. The size will be a trade-off between investment and operational cost and is depended on the temperature differences between the refrigerant and the surroundings, namely ΔT_c and ΔT_e for the condenser and evaporator respectively.

Investment costs:
If high ΔT; small heat exchanger can be applied. The compressor must be designed slightly larger. Overall lower investment costs compared to low ΔT.

Operational cost:
If high ΔT; High energy consumption, implies higher operational costs compared to low ΔT.

The correlation between ΔT and the size of a heat exchanger with a given effect can be derived from equation 3.1. For example, in the evaporator, Q is decided by the refrigeration capacity. The increase of ΔT_{LM} implies a reduction of A with respect to equation 3.1. When reducing A (size of the evaporator), the investment cost decreases. On the other hand, if ΔT_{LM} increase, the operational cost increase.

$$Q = UA\Delta T_{LM} \tag{3.1}$$

$$\Delta T_{LM} = \frac{\theta_2 - \theta_1}{(ln\frac{\theta_2}{\theta_1})} \tag{3.2}$$

$$\theta_2 = T_{hi} - T_{ci}, \theta_1 = T_{ho} - T_{co} \tag{3.3}$$

$$Q = \dot{m}\Delta h \tag{3.4}$$

Figure 3.3 display two different cycles. The green has a high ΔT and small heat exchangers. The red has low ΔT and large heat exchangers. It can be seen that the green cycle has a lower enthalpy change than the red in the evaporator. This must then be compensated for by increasing the mass flow (equation 3.4). Besides, the enthalpy change for the compressor is greater, which also increases operational costs. The red cycle will provide low operational costs and high investment costs, whereas the green will provide the opposite.

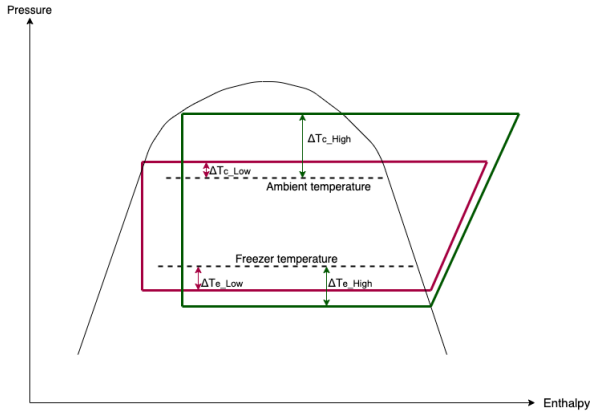

Figure 3.3

When the temperature differences have been decided, both the evaporation- and condensation temperature are locked. These temperatures have a corresponding pressure level. Since the pressure levels are known, a compressor can therefore be chosen. When determining the compressor size, it is important to know the mass flow to achieve the correct refrigeration capacity.

3.1.1 Coefficient of Performance

The purpose of a refrigeration cycle is to remove heat from the refrigerated volume. In order to determine the efficiency of the refrigerant cycle, a coefficient of performance (COP) can be calculated. COP is the ratio between the amount of heat extracted from the refrigerated volume ($\dot{Q}_{evap}$) and the electrical consumption ($\dot{W}_{tot}$). The COP for the refrigeration cycle defined by equation 3.5.

$$COP_{cooling} = \frac{\dot{Q}_{evap}}{\dot{W}_{tot}} \tag{3.5}$$

3.2 Ultra low temperature freezers

Ultra-low temperature freezers can contain temperatures of -40°C to approximate -86°C. There exist several different technologies to achieve these temperature levels. The typical design criteria for all these technologies are the freezer- and ambient temperature. To achieve this temperature difference, one or more pressure levels have to be implemented in the cycle. One such example is illustrated in figure 3.4.

3.2.1 Cascade system

A cascade system consists of two cycles with a compressor, evaporator, condenser, and a valve. The cycles are thermally connected to each other through a heat exchanger called the cascade condenser. As an example, the high-temperature cycle (HTC) uses ammonia (R717) as refrigerant, whereas the low-temperature cycle (LTC) uses carbon dioxide (R744) as refrigerant illustrated in 3.4. The log pressure - enthalpy diagram describing the system is shown in 3.5. Heat load from the freezer is absorbed in the evaporator in stage 4-1. R744 is compressed to state 2 before it rejects the heat to the HTC (R717) in the cascade condenser. This heat rejected from state 2-3 is absorbed by 8-5. R717 is then compressed from 5-6 before rejecting the heat to the ambient in the condenser.

The thermodynamic efficiency of this system is depended on the design of the different components and the temperature levels. According to Roul et al. (2014), maximum COP of approximate 2,0 can be derived with an evaporator temperature of -50°C and a condenser temperature of 30°C.

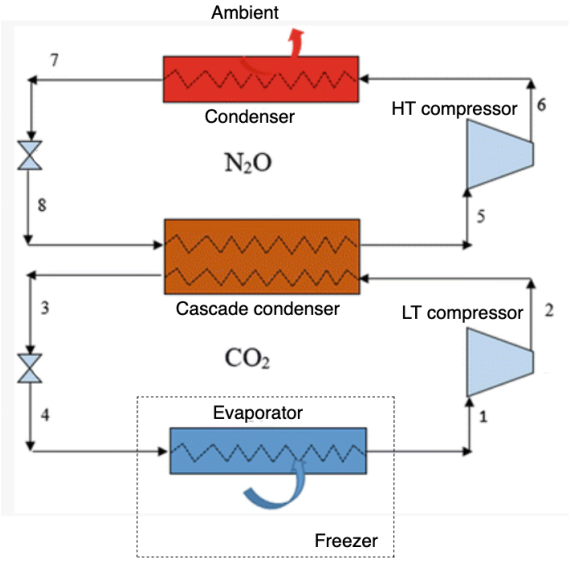

Figure 3.4: Cascade refrigeration system utilizing Ammonia in the HTC and CO_2 in the LTC (Yılmaz et al., 2016)

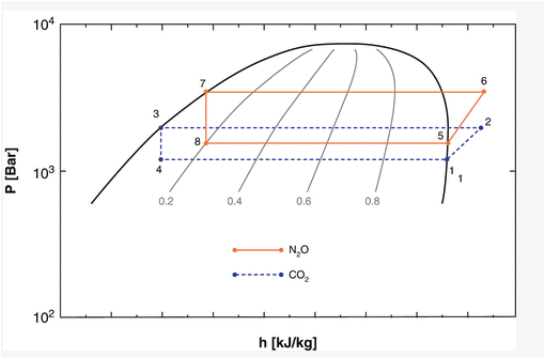

Figure 3.5: Cascade refrigeration system (Yılmaz et al., 2016)

3.2.2 Reversed Brayton

Another technology providing temperatures lower than -86°C is the reversed Brayton cycle. This cycle consists of an evaporator, a condenser, a turbine, and an expander. In a Brayton cycle, the refrigerant is at a gaseous state during all stages. According to a thermodynamic analysis performed by Streit and Razani (2013), an evaporator temperature of -100°C can be achieved with a COP of approximate 0.275.

In addition to the mentioned cascade system utilizing R717 and R744 and the reversed Brayton cycle, several other low freezing technologies exist. Due to the substantial tem-

perature differences between the ambient and the freezer temperatures, high-pressure differences must occur in the cycle, independent of the technology. This pressure difference is achieved by a compressor that requires electrical power. As the pressure difference increase, the power consumption increase. Because of this, the COP value decreases with the decrease of freezer temperature.

3.3 Air blast freezing

Air blast freezing cools a food product by use of air. Thus heat from the air is removed by passing it over an evaporator. The air velocity in the freezer is controlled by fans. Increasing the air velocity results in increased heat transfer coefficient between the food product and the air, thus reduction in the freezing time. An overview of different air blast freezers are presented below.

3.3.1 Batch Freezer

A batch freezer is a stationary air blast freezer where the products are placed in an insulated volume. Low temperature air circulates over the food products powered by fans. The products are stacked on pallets or hung from hooks. To achieve a uniform airflow speed in freezer, there are arranged spacers between the layers. This is important to avoid large variations in the cooling rate between different parts of the freezer and end up with consistent product quality for all food products in the freezer. A batch freezer is used for large products with irregular geometry and often different sizes. In a batch freezer, one batch of a product is frozen before a new batch replaces the frozen one. In a push through trolley freezer, a mechanical system moves racks through a tunnel in a cyclic manner. The freezing time is often difficult to predict in an air blast freezer due to often large variations of product size, shape, and composition (Johnston, 1994).

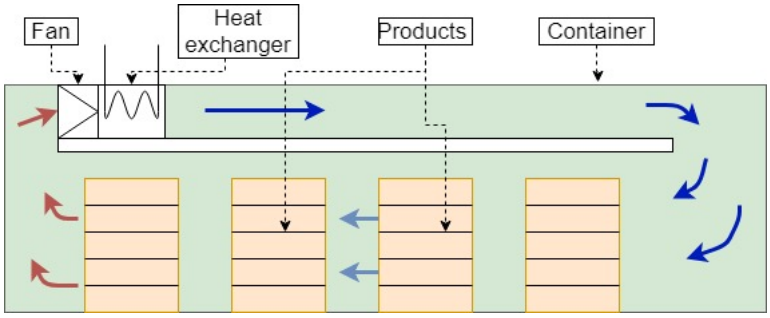

Figure 3.6: The figure shows a conventional batch freezer system

Figure 3.6 shows how the air flows through the trolleys stacked up of the product. In this particular figure, we see boxes of the same size, but they could have a different composition. A batch freezer has a low capital cost and versatile, but longer freezing time and low heat transfer coefficient.

3.3.2 Belt Freezer

A belt freezers use perforated belts to transport the products through the freezer. The air flows vertically on the products to force air between the products. To achieve proper freezing, it is important for the products to be evenly distributed across the belt. If not, ”channeling” will occur and result in poorly frozen products (Mallett, 1993; Dempsey and

Bansal, 2012). There are different types of belt freezers. Figure 3.7 shows a multi-tier freezer, and this type of freezer is useful when the space floor available is limited. It consists of several conveyor systems positioned on top of each other. These freezers are beneficial for small products of the same size.

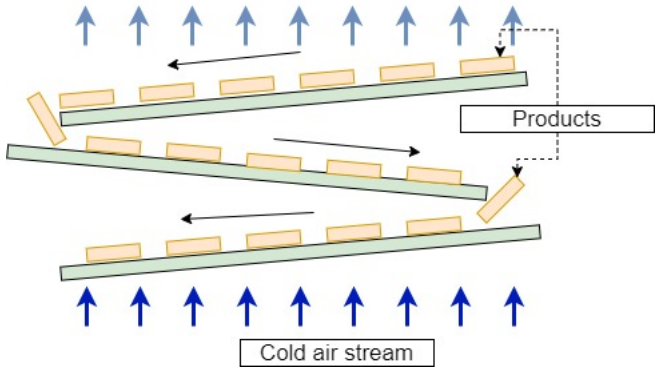

Figure 3.7: The figure shows a multi-tier belt freezer with vertical air flow.

Spiral Belt Freezers

Spiral Belt Freezers have the same belt structure as multi-tier, but the belt are coiled around a central axis several times with a certain height. This gives some advantages to operate small floor space area. Spiral belt freezer is more suitable than normal belt freezer for products that have longer freezing time.

3.3.3 Fluidized Bed Freezers

Fluidized bed freezers consist of a mesh conveyor belt where cold air streams upward in a vertical direction. A fluidized bed freezer is used to freeze products with specific uniform size and shape, such as berries, peas, or chopped vegetables. The air velocity is so high that the food product begins to float and jumps up and down. It gives a very low freezing time because the jumping exposes all sides of the product to the cold air (Johnston, 1994). Figure 3.8 shows how a fluidized bed freezer works. The yellow dots represent food products that jump around.

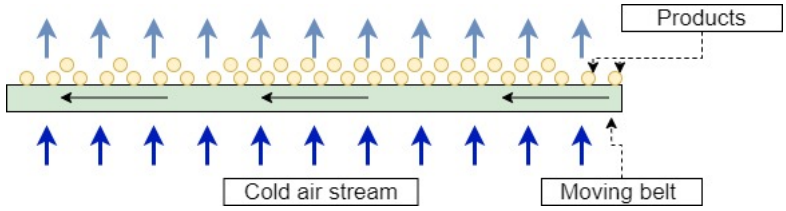

Figure 3.8: The figure shows a Fluidized Bed Freezer

3.4 Cryogenic Freezers

Cryogenic freezing is a freezing process where the food is directly exposed to liquefied gases of either carbon dioxide (CO_2) or Nitrogen (N_2). The product's surface is sprayed with the liquefied gas, or the products are immersed into the liquefied gas. Cryogenic freezing has low freezing time compared the air blast freezer due to the vast temperature difference between the products and the cryogen. The system is most effective on small products such as berries and small fruits. The operational cost is high due to the cost of the refrigerant. (Goswami, 2001; Sun, 2016). In figure 3.9, liquefied nitrogen is sprayed on to the products which are transported on a belt.

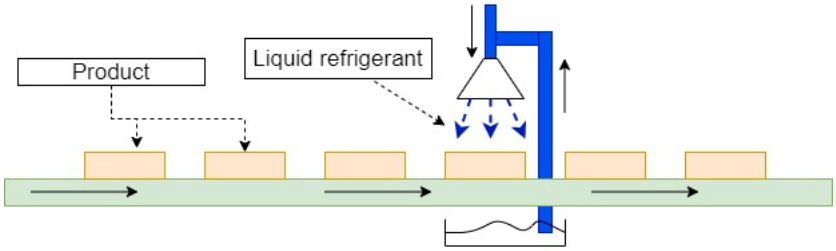

Figure 3.9: Flow scheme of a Liquefied Cryogenic Freezer

3.4.1 Immersion Freezers

The immersion freezer, freeze products by immersing them in liquid nitrogen. This method provide a the highest heat transfer coefficient than any other air freezing method. The products are transported on a belt through the bath of liquid nitrogen at -196 °C. Products are frozen to crust pieces. The advantage with immersion freezers is that the product can be irregular and complex in shape. If the immersion freezer is not operated correctly, the product surface may crack due to internal stress (Valentas et al., 1997; Sun, 2016; Goswami, 2001).

3.4.2 Plate Freezers

Plate freezers are commonly used for freezing fish or regularly shaped blocks and packages. There are two main types of plate freezers; the vertical plate freezer and the horizontal plate freezer. Plate freezer is space-efficient and is therefore often used offshore on the fishing boats. The advantage with plate freezers is the high heat transfer coefficient. This is due to product is in contact with the metal plate, which has excellent conductive properties. There is also low energy consumption since pumps, instead of fans are utilized. The products in a plate freezers require a specific size and shape which enables them to have a large contact area to the plates. Also, there are limitations to how low the temperature can reach because the refrigerant is a liquid than must not solidify. There are no refrigerants that can both operate at -25° and -70°C as a liquid. Glycol can reach -40°C in

circulation without freezing (Tolstorebrov, 2019). Glycol has a high thermal capacity, and the minimum temperature can be lower than other fluids (Goswami, 2001; Sun, 2016).

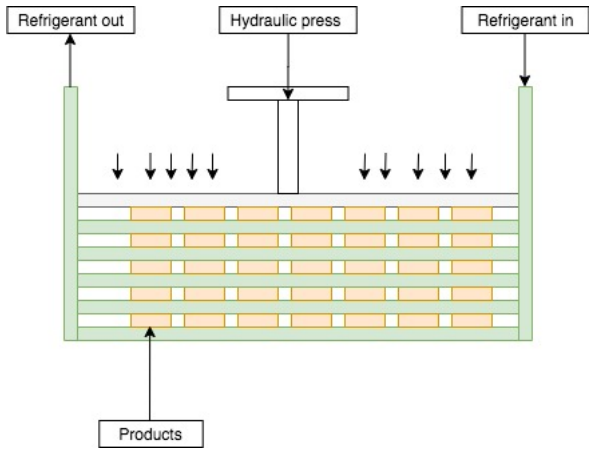

Figure 3.10: The figure shows a horizontal batch plate freezer

Figure 3.10 shows a horizontal batch plate freezer that consists of several layers of plates. The bottom layer plate is first loaded with products, and once it is full, a new plate is laid on top of it. This new plate is then loaded with products. After the products are frozen, they get unloaded, and a new batch is loaded.

3.5 Summary Freezing Technology

When developing freezer design, consideration of the correct freezing process for the food product is essential. Air blast freezer is the most common technology to use when freezing fish (Widell, 2020) in Norway. This is because it has low investment and operational costs, and are flexible to the fish size and shape. Cryogenic and plate freezers are not that often used despite higher heat transfer rates. In table 3.1 some key differences between air blast, cryogenic, and plate freezers are illuminated.

	Air Blast Freezer	Cryogenic Freezer	Plate Freezer
Flexible with respect to product size and geometry	High flexibility	Medium flexibility	Low flexibility
Operational complexity	Medium	High	Medium
Freezing temperature range	High range: +5°C to approximate -90°C	Low temperatures: -196°C to -50°C	Low range: +5°C to -40°C
Heat transfer rate from product / freezing time	Low/medium	Very high	High
Space requirement	High	Low	Low

Table 3.1: Comparison of the different freezing technologies

3.5.1 Refrigerants

A refrigerant is used for transporting the thermal energy from the source to a heating system by going through different states in a closed loop. The important factors when choosing a suitable refrigerant for the freezing system are safety, environmentally friendly, the physical and thermodynamic properties, temperature interval, and the cost. Several refrigerants and their properties are listed below.

Air (R-729)	Pros; Environmental friendly, non-corrosive to equipment, capable of a broad range of temperature applicability (-213.15 °C to 172.86 °C). Cons; Low COP and large system size.
Nitrogen	Pros; Environmental friendly, does not carry moisture, inert gas (which means it does not react with other materials) Cons; Low COP, very much the same as air.
CH_4 (R-50)	Pros; low refrigerant charge, low boiling point of -162 °C. Cons; very flammable.
C_2H_4	Pros; non toxic, low cost. Cons; Combustible

3.5.2 Regulator

A regulator is essential for a freezer to function and to control the freezing process. It registries the temperature in the freezer and adjusts it to the desired value by regulating the input power to the fan in the freezer. The power input results in specific air velocity and a specific heat exchange coefficient in the heat exchanger. Therefore, by regulating the fan power, the heat exchange in the freezer can be controlled, resulting in a regulation of the freezer temperature.

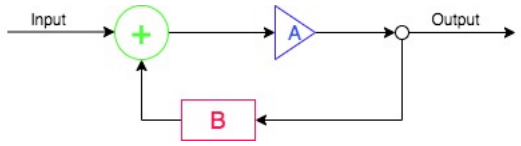

Figure 3.11: Feedback system

Figure 3.11 displays a simple freezer with a regulator. B is a sensor that registries the freezer temperature. The deviation between the freezer and the desired temperature is calculated in the green circle. Finally, the deviation is given as input to the regulator illustrated as the blue triangle, which calculates the output data to the fan. The process continues until the desired temperature is achieved, and the deviation is zero. The system described is called a feedback system.

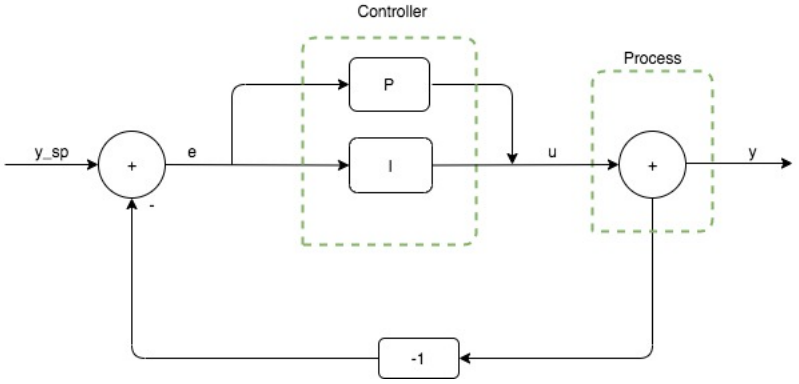

Figure 3.12: Block diagram of a control loop feedback system with a PI-regulator

The proportional-integral (PI) regulator consists of a more complex feedback system. Figure 3.12 displays a feedback system with a PI controller. The Proportional term (P) depends on the present error, and the Integral term (I) eliminates steady-state offsets by accumulate past errors (Åström and Hägglund, 1995). The system loop has the desired temperature (y_{sp}) and a registered temperature (y). The difference between y_{sp} and y is the deviation (e).

Chapter 4

Theoretical aspects of fish freezing

Historically, various methods have been used to conserve fish. Many of them are still used today, mainly driven by customer demand for processed food. An example of this is the conservation of unsalted dried fish, also known as Stockfish. The Stockfish is dried in cold air and can be conserved for many years. Other methods are salted fish and dried fish (clipfish), the burial of fish, and combinations of the mentioned methods. Freezing of fish is also a method that has been used over the years and is the most common today. The freezing of a fish inhibits the growth of most bacterial species and slow microbiological processes. There are specific characteristics of a fish that determines the quality. Fresh fish is of the highest quality, but the decomposition process starts immediately after death. Therefore, the fish has to be conserved during transport and possible storage to where it shall be consumed. Quality measurements such as texture, flavor, aroma, shape, and color should be conserved as best as possible. This is achieved by high-quality processing of the fish, which implies, among others, proper handling and quick freezing. To determine the storage stability of a food, the glass transition phenomena along with water activity, chemical and physical changes must be considered.

In this chapter, the principles of heat transfer and methods to calculate freezing time is introduced. Also, thermophysical properties and the geometry of a tuna is presented. Finally, the freezing process and how the freezer conditions affect the fish properties are established.

4.1 Heat Transfer

Heat can be transported by three different phenomenons: conduction, convection, and radiation. Radiation is negligible in a freezer and will not be elaborated. The freezing time is defined as the time it takes from the fish is placed in the freezer until it reaches the freezer's temperature. Heat is removed from fish during the freezing process. Factors that affect the freezing time are the following:

1. The Temperature of the freezer
2. The temperature of the fish
3. Thermal conductivity of the fish
4. The geometry or thickness of the fish - large area versus volume is desirable
5. Heat transfer rate from freezer to fish (either convection or conduction - depending on the freezer design)
6. Enthalpy change of the fish from initial temperature to freezer temperature

4.1.1 Conduction

Thermal conduction is defined as the transport of the internal energy of particles within a medium, e.g., solid, liquid, or gas. The temperature level of a particle is proportional to the internal energy of the same particle. During thermal conduction, particles in the medium collide, and energy is exchanged from the particle with high energy to the particle with lower energy. If external heat transfer is absent, the temperature difference in the medium will decrease by time before it reaches thermal equilibrium - a uniform temperature throughout the medium. The rate of which heat is transported by conduction is depended on the temperature difference- and the conductive properties of the medium. The heat transfer rate is defined by Fourier's law equation 4.1.

$$q = -k\nabla T \tag{4.1}$$

4.1.2 Convection

Convective heat transfer is defined as the transfer of heat by the movement of one or more fluids. Convection is the dominant heat transfer in liquids or gases but also occurs between solids and fluids. When a fluid flows over a solid of different temperatures, heat will be transferred at the surface. This fluid flow can either be natural or forced by e.g., a fan or pump. Forced convection reaches higher heat transfer rates due to the fluid is transported away from the surface fast, enabling downstream fluid to exchange heat with the surface. The rate of heat transfer by convection between a solid and a fluid is depended on the heat transfer coefficient (h) and temperature difference. The rate of heat transported by natural convection can be expressed by equation 4.2. T_s represent the temperature at the surface and T_∞ represent the freezer temperature.

$$\frac{d(Q)}{dA} = -h(T_s - T_\infty) \tag{4.2}$$

4.1.3 Heat equation

The heat equations follows from the physical laws of conduction, convection and radiation. To calculate the freezing time for a tuna, the heat equation can be applied. For a closed homogeneous, isotropic plane with no heat generation or radiation heat transfer, equation 4.3 can be derived:

$$\frac{\delta T}{\delta t} = \alpha \left[\frac{\delta T^2}{\delta x^2} + \frac{\delta T^2}{\delta y^2} + \frac{\delta T^2}{\delta z^2} \right] \tag{4.3}$$

where α is the diffusitvity and is defined as:

$$\alpha = \frac{k}{c_p \rho} \tag{4.4}$$

4.2 Application of heat equation

The heat equation describes the correlation between temperature, distance, and thermodynamic properties of a volume. There exist several numerical approaches to solve the heat equation for a given volume.

4.2.1 Discretization

One approach to solving the heat equation is to establish a mesh of nodes that describe the geometry of the volume. A node is a point in space with zero dimensions, described by its coordinates. The node can be applied thermophysical values, e.g., temperature. To be able to solve the heat equation numerically, the elements $\delta T^2/\delta(z)^2$ (z is a distance in space) of equation 4.3 must be discretized. The discretization enables the use of computer programs to calculate the temperature change with time for each node.

The heat equation can be discretized by using a central differentiation in space with one-time step forward. This method is called "forward in time, center in space" (FTCS). To illustrate, a 2D plane is shown in figure 4.1 where the goal is to calculate the new temperature of point P. The new temperature in point P is dependent on the old temperature to the points next to it, illustrated by the red arrows. Index n describes the n^{th} time step, with a time difference of dt between each step. Equation 4.5 calculates the new temperature of a general point (i,j) using FTCS.

$$T_{i,j}^{n+1} = T_{i,j}^{n} + dt \cdot \alpha \left[\frac{T_{i-1,j}^{n} - 2T_{i,j}^{n} + T_{i+1,j}^{n}}{(dx)^2} + \frac{T_{i,j-1}^{n} - 2T_{i,j}^{n} + T_{i,j+1}^{n}}{(dy)^2} \right] \tag{4.5}$$

In figure 4.1 the indexes i and j describe the number of stages (dx and dy) from orig for x and y respectively. The temperature of node P is affected by the nodes next to it, shown by the red arrows.

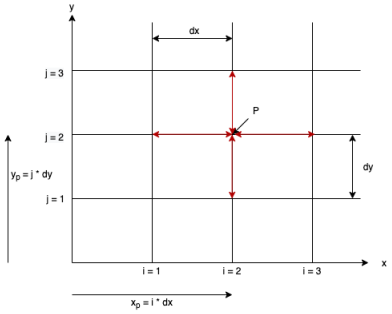

Figure 4.1: The figure display a coordinate mesh for a point P with length dx in the x-direction and length dy in y-direction.

4.2.2 Boundary and initial conditions

Notice that the equation 4.5 does not apply for nodes at the boundary; point along with i = 0 and j = 0 does not have four connecting points. In a physical model, the boundary can e.g., describe the surface of the object. The nodes at the boundary must, therefore, be given additional information, called boundary conditions to solve the equation. Moreover, the first time step has to be calculated by applying the initial temperature. The initial temperature distribution for the volume must, therefore, be given, called initial condition.

4.2.3 Radial geometry

If the volume has a shape of a rectangular box or similar geometry, equation 4.5 is the preferred method to solve the heat equation. All the nodes along the boundary (surface) exists and can be defined. However, if the volume is shaped like a cylinder, equation 4.5 is not preferred. This also applies to volumes with elliptic cross-sections, for example, tuna fish. Equation 4.5 is based on Cartesian coordinates, and it is not easy to describe the boundaries along the surface of a cylinder or ellipse. This is illustrated in figure 4.2.

To solve the problem, another method to define the nodes is utilized. By introducing polar coordinates, the mesh of a cylinder is simplified and improved. The x and y coordinates is replaced by r and θ defined by equations 4.6 and 4.7. The z-dimension is not changed and is the same as in Cartesian coordinates. The node can be applied thermophysical values, e.g., temperature.

$$r = cos(\theta)/x \tag{4.6}$$

$$r = sin(\theta)/y \tag{4.7}$$

The figure 4.2 mesh is divided to length dx in the x-direction and length dy in y-direction. The indexes i and j describe the number of stages (dx and dy) a node exists from orig. For figure 4.3, it can be noted that all the nodes along the boundary exist. Point P is described by θ and R coordinates.

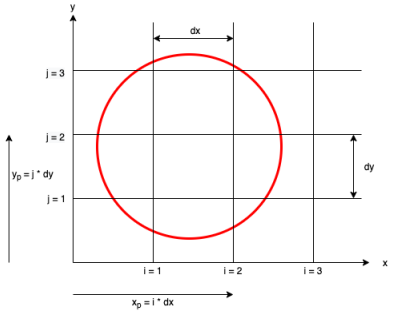

Figure 4.2: The figure display a coordinate mesh which is used to describe the geometry of the red circle.

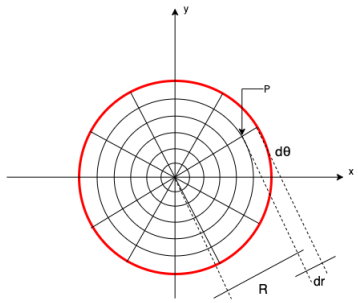

Figure 4.3: The figure has polar coordinates to describe the node inside a red circle.

By utilizing polar coordinates, the nodes in a cylinder can be illustrated, as shown in figure 4.3. The heat equation for a closed homogeneous, isotropic volume with no heat generation or radiation heat transfer, in polar coordinates, is described by equation 4.8. Following the FTCS scheme, the discretized equation is expressed by equation 4.9.

$$\frac{\delta T}{\delta t} = \alpha \left[\frac{1}{r} \frac{\delta}{\delta r} \left(r \frac{\delta T}{\delta r} \right) + \frac{1}{r^2} \frac{\delta T^2}{\delta \theta^2} + \frac{\delta T^2}{\delta z^2} \right] \tag{4.8}$$

$$\begin{aligned} T_{i,j,k}^{n+1} = T_{i,j,k}^{n} + dt \cdot \alpha \Bigg[& \frac{T_{i,j,k+1}^{n} - 2T_{i,j,k}^{n} + T_{i,j,k-1}^{n}}{dr^2} + \frac{1}{r_k} \frac{T_{i,j,k+1}^{n} - T_{i,j,k-1}^{n}}{2dr} \\ & + \frac{1}{r_k^2} \frac{T_{i,j+1,k}^{n} - 2T_{i,j,k}^{n} + T_{i,j-1,k}^{n}}{d\theta^2} + \frac{T_{i+1,j,k}^{n} - 2T_{i,j,k}^{n} + T_{i-1,j,k}^{n}}{dz^2} \Bigg] \end{aligned} \tag{4.9}$$

In figure 4.9 index i,j and k represents x-, theta (θ)- and radial (r) direction respectively, n represents the time step. r_k represent the distance from center to the node.

4.2.4 Biot number

The Biot number is defined as:

$$Bi = \frac{\alpha D}{k} \tag{4.10}$$

The Biot number is a dimensionless and represent the relationship between the internal thermal resistance D/k, and the external thermal resistance $1/\alpha$. If Bi is low (< 0.1), the internal heat resistance is much lower than the external heat resistance, which results in a surface temperature approximate to the core temperature. If $0.1 < Bi < 100$, both external and internal heat resistance have an impact on the heat transfer. There will be a smooth temperature gradient inside the product during freezing. If $Bi > 100$, the internal thermal resistance is significantly larger than the external. This is typical for large products where the surface to volume ratio is low.

For a tuna fish, it is intuitive that the temperature distribution inside the fish is not uniform. The Biot number can be calculated to be larger than 1 for any large tuna fish. This implies that no assumption of uniform temperature in the fish can be made.

4.3 Thermophysical properties of Tuna

The following formulas and data are extracted from (Kennedy, 2018). These equations are only valid to -40 °C. The largest variations occur near the freezing point, and as the temperature is close to -40 °C, the values converge. Below -40 °C, the values continues to converge (or stay linear) until a temperature of approximate -55 °C. At this temperature, the glass transition starts to occur and small deviations of the properties take place (Orlien et al., 2003).

4.3.1 Ice fraction

The ice fraction can be expressed by equation 4.11:

$$x_{ice}(t) = (x_{wo} - x_b)\big(1 - \frac{T_f}{T}\big) \tag{4.11}$$

where x_{wo} is the mass fraction of water above initial freezing point, x_b is the mass fraction of bound water, T_f initial freezing point of food (°C) and T is the food temperature (°C). The ice fraction increases with the decrease of temperature and is dependent on the composition of the Tuna.

4.3.2 Density

The density of the tuna fish is depended on the composition of the fish, as well as temperature. The mean value can be calculated for the different compositions.

Equation 4.12 to 4.16 calculates the density for protein (ρ_p), fat (ρ_f), ash (ρ_a), ice (ρ_{ice}) and water (ρ_w) of the fish, respectively.

$$\rho_p = 1.3299 \cdot 10^3 - 5.1840 \cdot 10^{-1} T \tag{4.12}$$

$$\rho_f = 9.2559 \cdot 10^2 - 4.1757 \cdot 10^{-1} T \tag{4.13}$$

$$\rho_a = 2.4238 \cdot 10^3 - 2.8063 \cdot 10^{-1} T \tag{4.14}$$

$$\rho_{ice} = 9.1689 \cdot 10^2 - 1.3071 \cdot 10^{-1} T \tag{4.15}$$

$$\rho_w = 9.9718 \cdot 10^2 + 3.1439 \cdot 10^{-3} T - 3.7574 \cdot 10^{-3} T^2 \tag{4.16}$$

4.3.3 Conductivity

Conductivity is calculated similar to the density. The conductivity of each composition is calculated. Equation 4.17 to 4.21 calculates the conductivity for protein (k_p), fat (k_f), ash (k_a), ice (k_{ice}) and water (k_w) of the fish, respectively. To decide the overall conductivity, the volume fraction for each element is derived by equation 4.22).

$$k_p = 1.7881 \cdot 10^{-1} + 1.1958 \cdot 10^{-3} T - 2.7178 \cdot 10^{-6} T^2 \tag{4.17}$$

$$k_f = 1.8071 \cdot 10^{-1} - 2.7604 \cdot 10^{-4} T - 1.7749 \cdot 10^{-7} T^2 \tag{4.18}$$

$$k_a = 3.2962 \cdot 10^{-1} + 1.4011 \cdot 10^{-3} T - 2.9069 \cdot 10^{-6} T^2 \tag{4.19}$$

$$k_{ice} = 2.2196 - 6.2489 \cdot 10^{-3} T + 1.0154 \cdot 10^{-4} T^2 \tag{4.20}$$

$$k_w = 5.7109 \cdot 10^{-1} + 1.7625 \cdot 10^{-3} T - 6.7036 \cdot 10^{-6} T^2 \tag{4.21}$$

$$x^v_{comp} = \frac{x_{comp}/\rho_{comp}}{\Sigma x_i / mean\rho} \tag{4.22}$$

In equation 4.22 comp is the index for water, ice, protein, fat, and ash. x_i is the mass fraction of the food components, and $mean\rho$ is the mean value of the density at the respective temperature.

Further, the conductivity depends on if the heat travels perpendicular or parallel to the fibers in the tuna fish. For parallel heat transfer equation 4.23 is used and for parallel equation 4.24 is used. These two equations have been found to predict the upper and lower boundary of thermal conductivity for most foods. In a tuna fish, heat travels both perpendicular and parallel to its fibers.

$$k = \Sigma x^v_{comp} k_{comp} \tag{4.23}$$

$$k = \Sigma \frac{1}{\Sigma x^v_{comp}/k_{comp}} \tag{4.24}$$

4.3.4 Diffusivity

The diffusivity is defined as equation 4.25 describes and measures the ability of a material to conduct thermal energy relative to its ability to store energy. Materials with high diffusivity values will respond quickly to changes in their thermal environment. Low diffusivity values will take a longer time to reach thermal equilibrium. The SI unit of diffusivity is m^2/s.

$$\alpha = \frac{k}{c\rho} \tag{4.25}$$

4.3.5 Effusivity

Effusivity is defined as equation 4.26 describes, which measures the materials ability to exchange heat with the environment. This equation can be applied to calculate the surface temperature of the tuna during freezing.

$$e = (kc\rho)^{1/2} \tag{4.26}$$

4.3.6 Enthalpy

Enthalpy is defined as the sum of internal energy and the product of its pressure and volume. In the situation of fish freezing, the enthalpy change is the sum of the heat transferred from the fish to the freezer. If the enthalpy change of a tuna is per time is known, the heat load can be calculated, which will be the design criterion for the freezer. Also, it is possible to predict electrical consumption and freezing time.

During the freezing of a tuna, the water change phase into ice. In this phase change, a high amount of heat exchange from the fish to the surroundings is required in a small temperature interval. The latent heat exchange occurs over a temperature interval because the water is bound to solutes in the fish. As the temperature decreases, water crystallizes, and the solutes increase in concentration. At a temperature of approximately -10°C, most of the water has crystallized.

Following the assumptions of the model mentioned in 4.2.3, the enthalpy is only investigated below the freezing point of -2.2 $^\circ C$. The initial enthalpy value is set to the freezer temperature. To describe how the enthalpy decreases, Chen (1985) method is applied, described by equation 4.27.

$$H = (T - T_r)\left[1.55 + 1.26 - \frac{(x_{wo} - x_b)L_0 T_f}{T_r T}\right] \tag{4.27}$$

where H is the enthalpy of food, T_r is reference temperature (°C), and L_0 is the latent heat of fusion of water= 333.6 kJ/kg.

4.4 Geometry of Tuna

The geometry of a tuna is depended on the age of the fish. Studies have been performed to investigate the length and weight of a tuna fish. Table 4.1 display the correlation between age and length of a Tuna fish (Restrepo et al., 2010). As shown, the tuna can grow old and large, but the most common size is assumed to be lower, between 20 kg and 250 kg.

The curvature of the fish can be described by three sets of equations, which result in a curvature displayed in figure 4.4. The curvature can be mirrored by the x-axis to illustrate the whole Tuna shape. The equations are extracted from (Xin ZhiQiang, 2013). Each body cross-section is an ellipse with major to minor AR at 1.5.

The shape of a tuna can be described by the curvature seen in figure 4.4. However, if the model is scaled, either to a larger or smaller tuna, the weight - length ratio must be correlating with table 4.1. Therefore, when scaling figure 4.4, it is essential to examine that the weight of the new model matches the empirical data from table 4.1.

Age (years)	Lenght (cm)	Weight (kg)
0	30	0.6
1	55	3.5
2	77	9.5
4	116	31.7
5	133	47
10	198	153
15	240	269
20	267	366
25	284	440
30	295	492
35	302	527

Table 4.1: Table showing the weight and length of a tuna for a given age

4.5 Freezing process

4.5.1 Freezing curve

In the freezing process, fish usually enters the freezer at a temperature between 0-4°C (Widell, 2020). The process can mainly be divided into three stages. The different stages are depended on the fish temperature.

1. Pre-cooling - Fish has just entered the freezer, and heat is removed from it. The temperature drops until a point below freezing temperature. This is displayed as point S in the freezing curve figure 4.5. At this point, the fish is supercooled, and the nucleus starts to form. A nucleus is required upon which an ice crystal can grow.

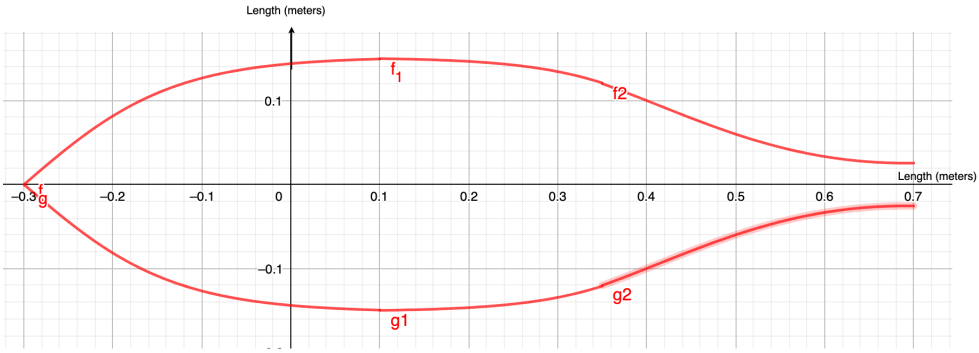

Figure 4.4: The figure display the tuna geometry seen from the side used in Matlab

2. Freezing - Further freezing results in the formation of ice crystals of the nucleus. The formation of ice crystals releases heat, leading to an increase in the temperature. The ice crystals continue to format, and the temperature drops slowly. In pure water, the temperature would be held constant until all water molecules would be ice crystals. In fish and other food, the temperature decrease as the crystals form because water molecules are bound to the solutes in the fish. Some of the water molecules will not freeze at a temperature below the freezing point. During the freezing, a solute can reach its saturation point, and all liquid freezes instantly.

3. Sub-cooling - Sensible heat is removed from the fish, lowering the temperature to the desired level. Normally this temperature is at -24°C. At this temperature, a small fraction of the water is at equilibrium with ice fraction. If the temperature is lowered to -60°C, most of the water has turned into ice crystals, and the rest is at a glass phase. The glass phase and the ice crystals reduce the biological and chemical processes compared to conventional freezing at -24°C, thus improving the conservatives of the fish.

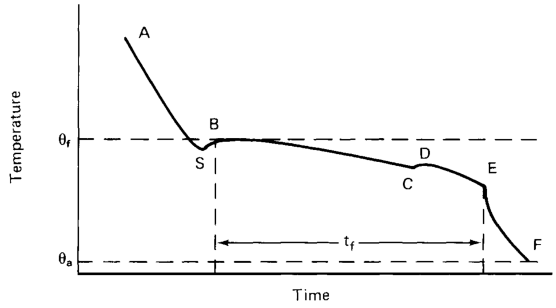

Figure 4.5: Time-Temperature diagram, the curve is known as freezing curve for fish (Fellow, 2000).

Each step of figure 4.5 is described below:

AS	The removal of heat decreases the temperature to state S below 0°C. The water remains liquid nonetheless, the phenomena is known as supercooling.
SB	Temperature rises due to the heat generation of ice crystal formation.
BC	Latent heat is removed, the temperature remains almost constant due to ice formation. The reason why the temperature drops slightly is because the solutes concentration increases in the unfrozen water, prohibiting it to freeze at 0°C.
CD	One of the solutes become saturated and crystallises. The latent heat of this process is released, resulting in a temperature increase.
DE	Crystallization of water and solutes continuous.
EF	The temperature decreases to the temperature of the freezer. At -20°C, approximate 91% of the water has frozen in fish (Fellow, 2000).

4.5.2 Formation of ice crystals

Before an ice crystal can form, a nucleus of water molecules must be available. A large number of nuclei is produced during high rates of heat transfer, and few during low rates. These two heat rates lead to respectively many small and few large crystals. Large crystals will puncture the cells where they grow, whereas small crystals can form inside the cell, without puncturing the cell. After thawing, the fish will have worse quality if it had endured prolonged freezing versus a fish that had a short freezing time. As the temperature decrease, individual solutes reach their saturation point and crystallize. The final eutectic temperature is defined as the lowest temperature where maximum ice crystal formation has occurred.

4.5.3 Water activity

Micro-organisms can deteriorate food rapidly, whereas enzymic and chemical reactions can take place more slowly during cold storage (-24°C). The deterioration rate of the fish is highly dependent on the water content. The water content is not sufficient to determine the shelf life of food, but also the availability of water. The availability of water is measured by the water activity, also known as Relative Vapour Pressure (RVP). The water activity is defined as 4.28 and depends on:

1. The amount of water present
2. The temperature
3. The concentration of dissolved solutes (particularly salts and sugars) in water

$$a_w = P/(P_0) \tag{4.28}$$

P is the vapour pressure of the food and P_0 is the vapour pressure of pure water at the same temperature.

A fraction of the water in a fish is bound to components such as salt, acid, and other natural compounds. Some of this bound water does not freeze even at low storage temperatures. The movement of the water vapour from the fish to the surroundings is depended on the food (moisture content and composition) as well as the temperature and humidity of the air. If the surrounding air is held at stable conditions, the moisture content of the fish will change until it reaches an equilibrium with the surroundings, known as equilibrium moisture content.

The effect of relative water activity on food is described in figure 4.28. It gives an indication of the effect of the water activity and will vary from different fish species. Most microbiological and fungi activity is inhibited below a_w= 0.7. There is little bacteria activity below a_w = 0.9. Chemical changes, such as browning and oxidation of lipids, occur during low relative water activity. Water is a product of the browning process, and at high moisture content, the browning process decreases (Fellow, 2000).

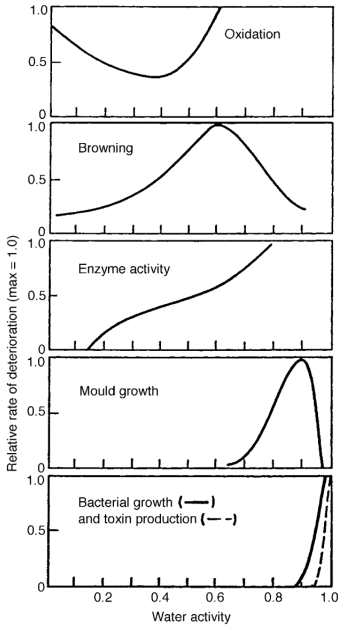

Figure 4.6: Water activity plot against relative rate of deterioration in different deterioration processes (Karel et al., 1975)

4.6 Operational conditions of freezers

Different temperatures and velocities in an air blast freezer result in different freezing temperatures, freezing load, and freezing time. It is essential to consider these parameters when designing a freezer to ensure that the product quality is preserved during storage.

4.6.1 How freezing time effect fish quality

As explained in 4.5.2, high amounts of ice crystals are desirable to avoid puncture of cells. The formation of many small ice crystals is achieved by short freezing time. If seafood is frozen incorrectly, effects such as off-flavor, rancidity, dehydration, weight loss, loss of texture, and toughening can occur (Valencia-Perez et al., 2015).

A study has been performed to investigate two different samples of mackerel, frozen in a commercial plate and air blast freezer. The fish was placed individually in a fibreboard carton before freezing. The freezing time was significantly different for the two methods, 90 and 220 minutes for plate and air blast freezer, respectively. Moisture content decreased in the air blast freezer compared to the plate freezer. During freezing and throughout the storage, lipid oxidation products and volatile bases showed slightly higher values of air blast freezer than of plate freezer. Also, the air blast freezer had higher values of histamine and fat-oxidized and products than plate freezer. The taste and satisfactoriness of the fish were significantly different in plate freezer compared to the air blast freezer upon three months of storage (Lakshmisha et al., 2008). Similar results were found in (Crigler and Dawson, 1968).

Other investigations suggest that rapid freezing minimizes damage on cells because the ice crystals were able to form in the intercellular spaces. Fish fillets were frozen at the different freezing times, and the ice on the muscle was studied by the deoxyribose nucleic acid method. The rapid freezing time was 115 minutes, compared to the average freezing time at 200-500 minutes and slow freezing at approximately 750 minutes. During the rapid freezing, the cellular damage was low; ice was formed in the intercellular space. The maximum cell damage was observed at the average freezing time before it decreased (Love, 1958).

Another study has been made that compares the air blast freezer at -28°C with cryogenic freezing using liquid nitrogen as a refrigerant. The food that was processed was shrimps. The freezing time, the weight loss during freezing and cutting force is displayed in the table below. The cutting force is applied after thawing. An optimal velocity in the air blast freezer is 6 m/s, whereas there are small differences between the different cryogenic temperature levels (Boonsumrej et al., 2007). Figure 4.2 shows how the scrimps described above change in a cryogenic freezer vs. an air blast freezer.

Freezing method	Freezing time (s)	Freezing loss (%)	Cutting force (N)
Air blast at air velocity			
4 m/s	371	2.71	19.3
6 m/s	363	2.14	21.4
8 m/s	333	3.43	22.5
Cryogenic at			
-70 °C	214	1.83	22.5
- 80°C	191	1.81	22.8
- 90°C	154	1.75	23.8
-100°C	116	1.75	18.6
Fresh shrimps			21.6

Table 4.2: Freezing time, freezing loss and cutting force at different freezing methods

4.6.2 How operational conditions affect freezing time

Tan and Fok (2009) investigated fillets of adult tilapia fish. An adult fish weights approximate 350 gram. The results are shown in the table 4.3 and 4.4. As shown, lowering the temperature and increasing the velocities decreases the freezing time significant.

Air velocity = 5 m/s	
Air temperature (C)	Freezing time (h)
-40°C	1.02
-35°C	1.23
-30°C	1.54

Table 4.3: Freezing time at constant velocities

Freezing temperature = -35°C	
Air velocity (m/s)	Freezing time (h)
3	1.58
4	1.38
5	1.23
6	1.12

Table 4.4: Freezing time at constant temperature

4.6.3 Glass Transition

An amorphous material can reach a glass state at a specific temperature. An amorphous food can be formed by cooling (water crystallizes) and is not at thermodynamic equilibrium. The amorphous food behaves as an extremely viscous glass, which is necessary for the molecules to crystallize. The glass state is a second-order phase transition. The glass transition occurs over a temperature interval, though it is often referred to as a single temperature, T_g. As the temperature of the food reaches T_g, many physical properties of the food change. The most important are a decrease in free molecular volume, a decrease of specific heat capacity, a decrease in thermal expansion coefficient. The free molecular volume referrers to the volume unoccupied by solid matter, where molecules can move freely. The glass transition occurs over a narrow temperature interval. Therefore, onset and

termination T_g values are observed (Bhandari and Howes, 1999). A glassy state can be considered as a solid solution. The state limits molecular mobility, increasing the stability of the food during storage (Roos, 2010).

4.6.4 Ultra low temperatures

The object of freezing fish at ultra-low temperatures is to preserve the quality better. Tuna fish is highly prevalent in Japan, and a standardized quality measure, known as ”K-value”, is widely used to sort the fish in quality range. The K value is a biochemical index based on nucleotide changes and is referred to as one of the freshness indices. In Japan, the common freezing temperature is -60°C, but there are few reports that state why this temperature is the optimal storage temperature. An experimental study has been performed to evaluate changes in K value, pH, and water state, including glass state during storage at various temperatures, the lowest of -86°C (Augustini et al., 2001).

The result was a linear reduced reaction rate of the K value with decreasing temperature ranging from -10°C to -70°C. The linear value of the reduced reaction rate per 10°C was approximate 2.2. The exciting findings from this study were the storage at -86°C, where the K value reaction rate was reduced approximately 20 times compared to -70°. This ”step” reduction occurred because the tuna fish in the experiment reached a terminated glass temperature. This study shows that the storage of tuna at -75°C or lower is a superior method compared to storage at -60°C. Other reports based on experimental results state that the glass transition temperature of tuna is -71°C (Inoue and Ishikawa, 1997), -74°C (Orlien et al., 2003) and -72°C (Jensen et al., 2003).

Chapter 5

System solution for tuna freezer

5.1 Practical considerations

Before presenting the solution of how the tuna freezer will be designed, some practical consideration needs to be mentioned. These considerations will be used as arguments for the solution.

5.1.1 Access to LNG

It is necessary for the freezer to have enough access to mass flow of LNG since LNG is the source of the freezing potential. If the mass flow of LNG is stopped or decreased, the freezer would also have to stop or decrease the freezing effect. The LNG is heated to NG and is used for industrial purposes, independent of the freezing load. Therefore, it is crucial that enough LNG can be accessed when required.

Location

When selecting where to put the freezer, it is necessary to build it at the same location as the LNG terminal. It is possible to transfer heat over some distance, but the cost will increase with the distance between the freezer and the LNG terminal. This is because heat transfer in pipes at low temperatures requires insulation and electrical consumption. Because of this, the freezer must be located in the same location as the LNG terminal. In Norway, there are 25 LNG terminals, all located in the coastal area. The large terminals are mostly distributed at the west coast, and some smaller in the north as well as south-east. These locations are close to where the fishing of tuna occurs, which is mainly at the west and north of Norway (Fiskeridirektoratet, 2019). As a consequence, fishing boats can unload the fish directly to the terminal, where they will be frozen.

LNG terminal size

As mentioned, the size of the LNG terminals varies. The small terminals do not operate the whole year, but only when the LNG is required. This is a problem for the operation of the freezer because the freezer will operate independently of the LNG mass flow requirements. Therefore, only the large LNG terminals will be considered due to their continuous operation throughout the year, as well as during the whole day. If the terminal is large, it will be possible to operate the freezer with a high freezing load. In figure 5.1 data collected from Gasnor and Mowi show the amount of LNG distributed to some of the largest terminals in Norway.

Terminal	Amount of LNG per year
Mosjøen	20 - 30 000 ton
Sunndalsøra	7 - 15 000 ton
Lista	4 - 10 000 ton
Valsneset	4795 ton

Figure 5.1: Amount of LNG delivered to different locations in Norway each year in ton (information collected from mail with Gasnor)

5.1.2 Ice formation on heat exchangers

Depending on how the freezer is designed, ice formation on heat exchangers can occur. If the freezer is designed as a conventional air blast freezer, there will be a heat exchanger located inside the freezer. In the freezing room, where the fish is located, moist air will be accumulated due to the water content of the fish. The moist air will enter the heat exchanger downstream of the fan. Since the freezer will operate at low temperatures ($< -70°\text{C}$), the formation of ice on the heat exchanger will occur. Therefore, defrosting the heat exchanger must be considered when designing a conventional air blast freezer. In a well functioning freezer, the defrost should not affect the operation of the freezer appreciable. One solution is to implement two heat exchangers in the freezer. The purpose of this is to defrost one heat exchanger while the other one is operating. When defrosting a heat exchanger, a liquid medium with a relatively high temperature $> 10°\text{C}$ is used. The liquid medium will transfer heat to the ice resulting in melting or sublimation of the ice crystals.

5.1.3 Size of freezer

Tuna fish is a relatively large fish with an average length of 2,0 meters and a weight of 200 kg (Restrepo et al., 2010). Handling the fish is, therefore, a challenge, and trucks are often used to transport the fish. The size of the freezer must be large enough to transport the fish in and out using a forklift or a similar machine. In addition, a given freezer size limits the amount of tuna fish it is possible to freeze at the same time. Since Tuna fish requires rapid freezing after capture, enough freezing space must be available to freeze a whole batch of tuna. In Norway, specific quotas are given to respective fishing boats. These quotas should be a design criterion for the maximum demand for freezer space. The tuna requires space between each other, with the purpose of decreasing the freezing time.

5.1.4 Scaling

The quotas of Tuna fish have increased significantly in the last years and are expecting to continue increasing as a consequence of proper management of the fish stock. It is therefore difficult to design a correct sized freezer, concerning today's demands and future predictions. Flexible design solutions, which are easy to scale up or down, are beneficial. The extra freezing volume should be cheap to produce, easy to implement and operate by the same principles as the present volume. If scaling is difficult and expensive, the freezing capacity is at risk of not meeting the freezing demand. This would result in a worse quality of tuna meat and loss of sale income.

5.1.5 Automation

As with most industries, the fishing industry develops to become more automated. Examples of this are new filleting machines that can process the fish before freezing. These machines cut operational costs because they reduce the need for labor costs. When designing a new freezer, automation should be a priority to simplify the freezing process as

well as to cut operational costs. The automated freezer is mentioned in chapter 3; freezing technology, mainly consist of moving belts, where the frozen product exits the freezer.

There are mainly three primary problems when automating the freezing process of tuna fish. First of all, the freezing time is considerable for a tuna fish and can be estimated to be at least 15 hours (calculations are elaborated later). Second, the tuna fish can vary in size, that result in different freezing time. A belt freezer is therefore not convenient. Also, the tuna fish is massive, an adult fish can weigh 500 kg (Restrepo et al., 2010). Any equipment that transports or stores the fish must withstand the weight from the corresponding amount of tuna fish.

5.1.6 Implementation to existing infrastructure

An LNG terminal exists of tanks used for storage of LNG and a vaporizer that regasify the LNG. Between the LNG storage tank and the vaporizer, LNG is transported in a pipe by a pump. This system is illustrated in figure 5.2. The correct integration of the heat exchanger that will be used for the freezer is a parallel coupling on the pipe between the LNG tank and the vaporizer, as shown in figure 5.3. By installing a mass flow controlled valve, displayed as the three-way valve in figure 5.3, the correct amount of LNG flow transported through the heat exchanger can be controlled.

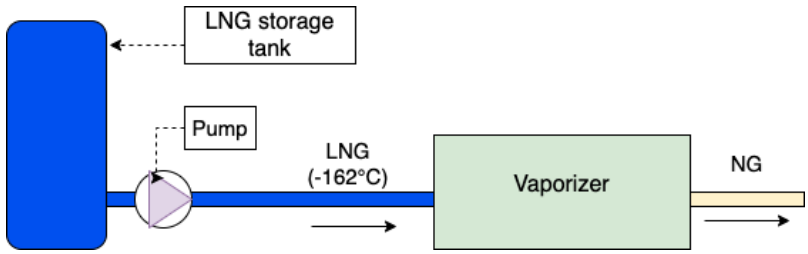

Figure 5.2: The figure shows components of an existing LNG terminal

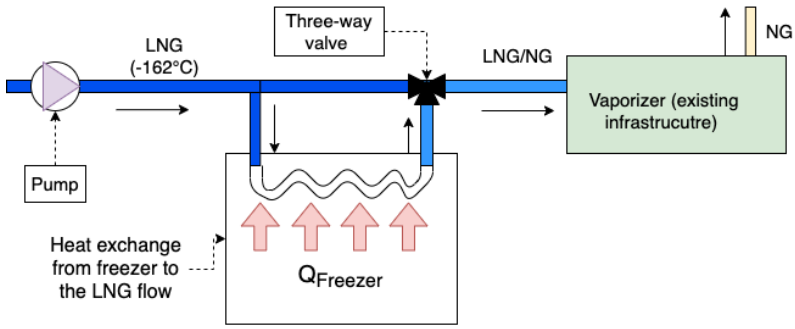

Figure 5.3: A coupling before the vaporizer is the correct way to integrate the freezer to the LNG flow

There are several benefits of installing the heat exchanger parallel to the pipe, before the vaporizer:

1. When the heat exchanger is placed upstream of the vaporizer, saturated liquid methane at -162°C (LNG) flows through the heat exchanger. The latent heat exchange at this temperature is of high quality for the freezer. If the heat exchanger is installed downstream of the vaporizer, the low-temperature freezing potential would be lost in the vaporizer, and the freezer would not reach low temperatures.

2. If the freezer requires high demands of freezer capacity, the three-way valve can be regulated to increase the LNG mass flow through the freezer system, seen as the white box in 5.3. Increasing the mass flow of LNG through the heat exchanger results in a higher freezer capacity to the freezer. A secondary effect of the increased freezing effect is lower heat exchange in the existing vaporizer. Vaporizers often require power consumption, and lower heat exchange results in lower operational costs of the vaporizer.

The only intervention that is necessary to execute on the existing infrastructure is the coupling of the inlet and outlet pipe on the LNG pipe between the storage tank and the vaporizer. This is a relatively small intervention and is cheap to perform. It can be performed on all LNG terminals and will not influence the operation of the gasification once installed.

5.2 System criteria

5.2.1 Temperature level

The freezer's objective is to preserve tuna fish at high quality. The glass transition temperature of tuna is approximate -73°C. As mentioned in chapter 4, glass transition increases the preservation of tuna compared to conventional freezing. The sale of tuna fish is potential a high value marked if the fish is preserved at ultra-low temperatures. Therefore, the motivation of preserving the tuna fish at glass temperature is economic gains for the parties that are included in the value chain, for example, fishers, salesmen, and transport companies. For the tuna fish to reach temperatures of -73°C or lower, a freezer temperature of maximum -80°C is recommended to keep the freezing time low. To decrease freezing time, freezer temperatures of -90°C or lower can be implemented.

Freezer temperatures of -75°C or lower will present some challenges to the system design. Typically, refrigerants operate as liquids or in the two-phase region. However, at temperature levels of -75°C to approximate -150°C (atmospheric pressure), no available liquid refrigerant exists. Therefore, mediums at gaseous state at these temperature levels must be utilized. Refrigerant gases have less beneficial thermodynamic properties than liquids, mostly due to low specific volume heat capacity; a high amount of volume flow must occur to transport heat.

Since LNG (-162°C) is used as a heat sink for the freezer, the freezer can operate in temperature levels of -80°C to -110°C.

5.2.2 Freezing capacity

The freezing capacity has to be able to freeze the amount of tuna fish that is unloaded to the fishing terminal. When boats are fishing for tuna, they usually capture large amounts at a time, since the tuna fish swim together in shoals. Therefore, large batches of tuna can arrive at once and needs to be frozen down simultaneously. The maximum freezing capacity there is possible to extract depends on the freezer size and the mass flow of LNG.

5.3 Choice of freezer technology

In chapter 3, existing refrigeration methods were elaborated. There are mainly three known concepts; plate-, cryogenic- and air blast freezers. The plate- and cryogenic freezer will not be investigated due to the following arguments:

Plate freezer

Plate freezers will provide high heat transfer rates, but this technology is not compatible with the requirements for the tuna fish. First of all, plate freezers cannot freeze the fish to the required temperature. Second, plate freezers will not cover the whole surface of the fish, due to the geometry of the tuna fish. Since the thickness of the tuna is relatively large, the heat resistance through the freezing process is highly dependent on the conductivity inside the fish. The plate freezers are more expensive compared to e.g. air blast freezers. Therefore, this will not be a part of the freezer solution.

Cryogenic freezer

The cryogenic freezer is possible to utilize and will provide a better heat transfer than the air blast freezer. However, the investment and operational costs are high. With access to LNG, the cryo-mechanical concept is the preferred solution. This installation requires a compressor, large heat exchangers, and high electrical power consumption for the compressor. For large products, like tuna fish, the cryogenic is often used to create a crusted surface, and then afterward continue the freezing in an air blast freezer. The freezer effect of a cryogenic freezer is very high at the beginning of the freezing process, but as the surface temperature decreases, the freezing effect is mostly dependent on the conductivity inside the fish (the same as with plate freezers). Therefore, a cryo-mechanical freezer would consume a high amount of electricity, and the result would only be some lower freezing time compared to an air blast freezer.

Air blast freezer

The air blast freezer is cheap, has low operational costs, and can reach low temperatures. It can freeze tuna fish of different sizes and is easy to build to withstand the heavyweight of the tuna fish. Trucks or other transportation devices must be able to load and offload the tuna fish. The appropriate air blast freezer for a tuna fish is the batch freezer. The other air blast freezers methods, using belts, are not suitable due to the size of the tuna fish. In Norway, approximately 90% of the fish freezers are air blast freezers (Widell, 2020). With the practical considerations and requirements for the freezer, two different designs have been investigated; indirect and direct heat transfer design.

5.3.1 Temperature and pressure levels

The constant pressure cycle is a simple system solution with few components. The heat is transferred from the fish to the LNG through mediums at atmospheric pressure. This freezer design deviates from the conventional freezer, explained in chapter 3.1, which

consists of two different pressure levels. The motivation of two pressure levels is to be able to exchange heat with the surroundings at the required temperature level. The surrounding heat sink for a conventional freezer is generally at ambient temperature, which in most cases are higher than the freezer temperature. The different pressure levels are therefore necessary.

However, in the investigated solution, LNG (-162°C) is used as a heat sink. Due to the low temperature of the LNG, there is no need for different pressure levels to reject heat. The difference in temperature between the tuna and LNG at the beginning of the freezing process is approximately 160°C. Even when the process is finished, the temperature difference will be a minimum 70°C. Because of these substantial temperature differences, the refrigeration system will not require a complicated design with several components. This will decrease the investment cost and simplify operational management.

5.4 Freezer design

Two different methods have been investigated, the indirect and direct design, shown in figure 5.4 and 5.5.

5.4.1 Indirect design

The first design solution 5.5, involves a closed loop with a refrigerant that absorbs heat in the freezer and rejects it to the LNG flow in a heat exchanger. The refrigerant must withstand low temperatures without liquefying or solidifying. Air, ethylene, and nitrogen are possible candidates that cannot liquefy in the respective temperature interval. As shown in the figure, two heat exchangers will be installed in the freezer. The reason for this is to solve the ice formation problem on the heat exchangers mentioned in 5.1.2.

The system is designed with two three-way valves. The valve at the top of the figure regulates the freezer capacity and also function as an on/off the regulator. If the freezer is shut off, the valve will control that no LNG flows through the heat exchanger, but directly to the vaporizer. The second three-way valve, placed in the closed cycle of the refrigerant, controls the flow through the two heat exchangers in the freezer. The valve is installed to manage the defrosting of each heat exchanger. The defrosting cycle is not shown in the figure but is connected to each of the heat exchangers in the freezer.

A PI controller is connected to the fan in the freezer. A temperature sensor located downstream of the fan provides input data to the controller, which signals the amount of power delivered to the fan, ensuring that the freezer temperature is kept at the desired level. Without the controller, there would be challenging to regulate the freezer temperature, and the power consumption would be higher.

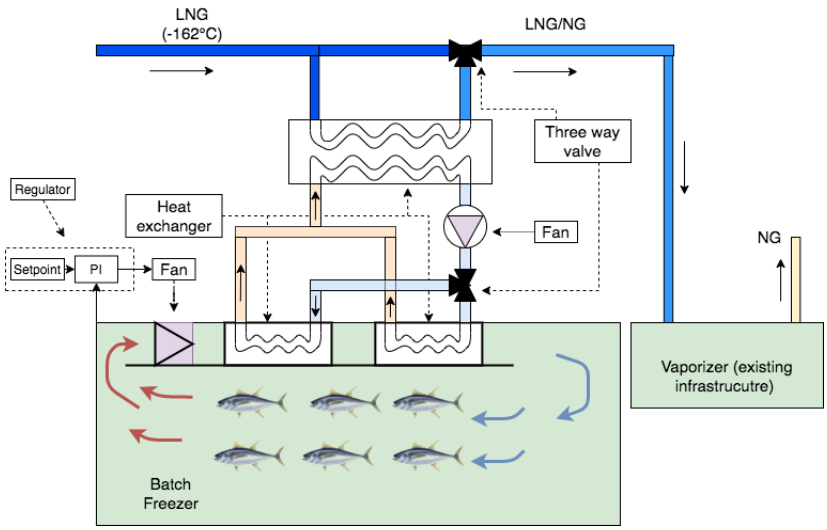

Figure 5.4: Indirect design: Heat transfer from freezer via a refrigerant to LNG

5.4.2 Direct design

For the second design 5.5, LNG is transported through the heat exchanger in the freezer. This results in a direct heat transfer from the air in the freezer, to the LNG. There are installed two heat exchangers with the same purpose as the indirect design - defrosting the heat exchangers. The same controller is also applied, regulating the freezer temperature. The system is design with the same amount of three-way valves as indirect design. Where the upper valve regulates the mass flow of LNG. If there is no need for freezing the valve will control that no LNG flows through the heat exchangers, but directly to the vaporizer. The second three-way valve controls the flow through the two heat exchangers in the freezer. The valve is installed to manage the defrosting of each heat exchanger.

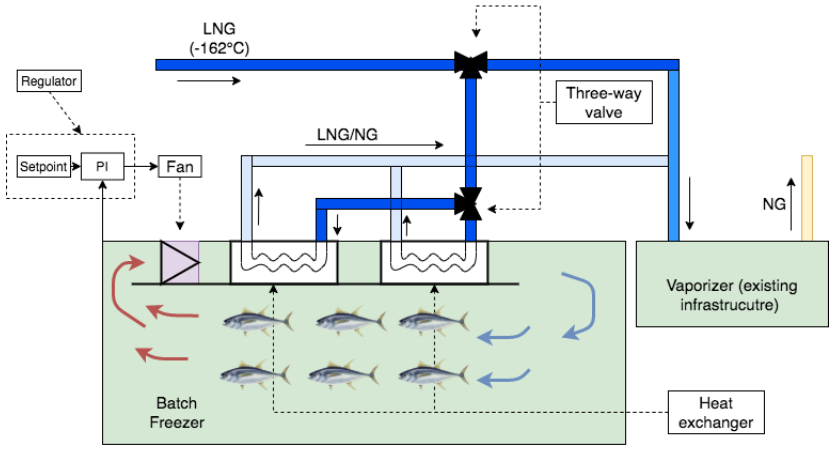

Figure 5.5: Direct design: Direct heat transfer of from freezer to LNG

5.4.3 Facility and storage capacity

For both methods, a container will function as the freezing facility. Containers are cheap to produce with the necessary insulation. In addition, it is easy to scale if the freezer capacity has to be increased or decreased by adding or reducing the number of containers. Also, a container does not require any intervention to the existing facility; it can be placed wherever suited and moved if necessary. The tuna fish will be placed on pallets before transported by a forklift into the container. The pallets are designed to place multiple tuna fish above each other. A sizeable insulated container has inside dimensions of 11.6 meters long, 2.3 meters wide, and 2.6 meters high.

5.5 Tracking of the Tuna

Once a tuna fish is caught, it has the potential to become a high-value fish. Japan consumes 90% of blue finned tuna (Ottolenghi, 2008a). The price per tuna in Japan can reach high values and is highly dependent on the quality of the fish, as mentioned in the introduction. Therefore it is essential to establish business connections to Japan to be able to export the fish. When fishing blue finned tuna in the USA, brokers in the USA and auction market official from Japan grade the fish from A-E (A represents the highest and E lowest grade) to assist the buyer in the purchasing decisions (Carroll et al.). This grading system only includes the freshness, fat content, color, and shape of the fish. The system is built on trust between the fisher, the people grading the tuna fish, and the buyer.

To build a successful trading platform, trust between the different actors involved is the critical factor. To develop such a system, a tracer will be marked on each fish. The tracer is a laminated paper, consisting of a QR code. The QR code can be scanned/accessed by an application on a smartphone, and the information about the fish will be given. Only people with authorization can add or change the information. Experienced marked offi-

cials from Japan, in combination with Norwegian brokers, will grade the fish in the same way as in the USA. This grade will be saved to the application and can be seen by anyone if the tracer is scanned. In addition to the grade, the description of every process the fish has undergone will be given. This includes the quality parameters listed above, such as freezing storage temperature and time from capture until freezing. This information is added to the application by trustworthy people and will be controlled frequently to avoid corruption or counterfeit of the information.

Chapter 6

Method

6.1 Predefined thesis

Before the thesis was defined, there were many concepts to choose between. The freezer could initially be used for several fish species and other food products. Information on fish quotas, the quality demand, rates of heat transfer, and the amount of LNG were evaluated.

There was much information about different fish species and their quota in Norway at Fiskedirektoratet.no. Moreover, SINTEF was contacted, and there were held a meeting with experts on fish freezing.

Furthermore, owners of LNG terminals were contacted, such as MOWI, Gasnor, and Barents Naturgass. Information on how the LNG terminals were operated and the amount of LNG that was consumed was collected.

6.2 Calculations performed in Matlab

Matlab is a programming language based on matrixes - allowing natural expressions of computational mathematics. The language has several built-in functions that enable agile approaches to arrive at a solution (Mathworks). Matlab was used to compute the freezing load and freezing time of a tuna fish

The FTCS scheme was used to solve the heat equation. To evaluate each node, three loops were implemented to cover the dimensions in space. In addition, one loop was dedicated to each step in time. Other self-made functions such as distance between each node, logical assessment if the node was located on the surface, and the thermophysical properties were implemented in the function.

To evaluate the core temperature of each time step, the function ”max” was used. The function finds the highest number in a vector. By applying the function on the temperature matrix, the core temperature was found.

To find the heat load from the fish, the temperature for each node was evaluated and given a specific enthalpy value. Furthermore, the mass of each node was found by calculating the volume multiplied with the density. The total enthalpy was calculated by multiplying the mass of each node with the corresponding specific enthalpy. All the enthalpy values were summed up and subtracted by the total enthalpy from the previous step, hence, finding the heat load effect. This value is added to a vector that consists of the effect at each time value.

6.3 Dymola

Modelica is an object-oriented and equation-based language that is used for modeling complex physical systems. Using Modelica enables us to model the dynamic behavior of a technical system with various components. The Modelica simulation environment used in this thesis was Dymola, TIL version 3.5.0. TIL enables the modeling of thermal systems.

To visualize the simulation results, software, DaVE, generated thermodynamic state charts for the fluids such as p-h-, p-v- and T-s diagrams.

The Modelica simulation environment, Dymola, was used. In Dymola, there are different components that are listed in the following table.

- VLEFluids - Green color and is compressible two-phase fluids; vapor/liquid and pure substances/mixtures
- Gases - Orange color and is an ideal gas/ gas mixture
- Liquids - Blue color and is incompressible single-phase fluids.

For this thesis, two models have been build in Dymola by ready-to-use components. One refrigeration design will have two heat exchangers, which exchanged cold from LNG

to air. The other system has an indirect cooling process, where a working fluid is first cooled down by a heat exchanger with LNG, and then the working fluid flows into a new heat exchanger where it is exchanging cold with air from the freezer.

Model building

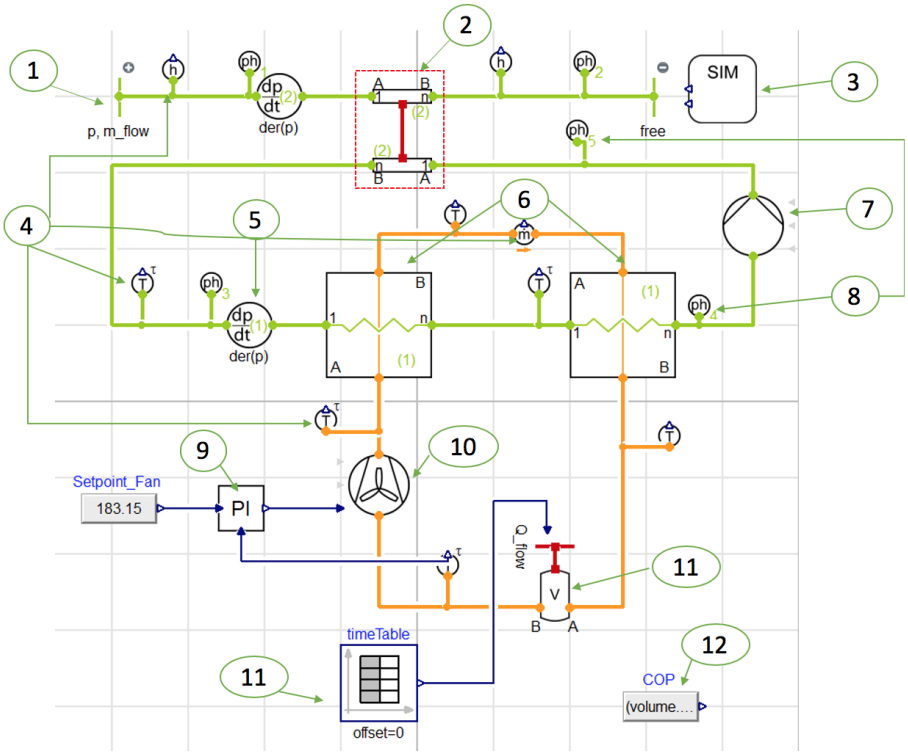

Figure 6.1: Dymola design model of the Indirect freezer system for tuna fish freezing

In figure 6.1, the design solution described in 5.3.1 are presented. It shows indirect design in Dymola. The green lines represents fluid refrigerants, and the orange line stands for a gas refrigerant. Furthermore the model consists of two fin and tube cross-flow heat exchangers, PI-controller, multiple sensors (mass flow, temperature, state points, enthalpy), two pressure states, SIM, boundaries, timeTable, and a simple heat exchanger. Which are all shown in figure 6.1 and are further presented below:

1. Boundaries	The VLEFLuid boundaries determine mass flow rate and temperature input. It was set to 0.1, 0.2, 0.3, 0.4 all up to 1 kg/s. The boundary output, after the heat exchanger, was free, which means that there are no constraints determined before the simulation.
2. Simple HX	A simple heat exchanger was designed with two tubes and a heat port since there was not a cross-flow heat exchanger with only VLEfluids. This was made. It only considers heat transfer between the fluids and nothing else. The heat transfer was set to 2000 W/K for the upper tube and 333 W/K for the lower tube. The geometry in the simple heat exchanger was the same as the geometry in the two other heat exchangers presented below.
3. SIM	A system information manager (SIM) was installed, and it defines the working fluids which are being used in the components for the designed system. Air, nitrogen, methane, and ethylene was used in this master thesis.
4. Sensors	Sensors with temperature, mass flow rate, and enthalpy were used to provide an overview during the simulation.
5. Pressure State	Pressure state was added for the simple heat exchanger and another one for the two fin and tube heat exchangers. They were sat at 1 bar.
6. Heat Exchanger	Two heat exchangers, which were cross flow fin and tube with the same geometry and arrangements, which are shown in **Appendix A**:(10.1,10.2). They were both not considering moisture in the heat exchanger.
7. Pump	Pump was used in the closed VLEfluid loop to control the mass flow. It was set to 5, 10 and 15 kg/s.
8. State point	State point was used for quickly understanding how the process evolves when evaluating how the enthalpy is changing.
9. PI	PI controller was used to control the mass flow of the airflow through the freezer. PI-controller has a Setpoint_Fan, which is an input of the temperature value set to 183.15 Kelvin. Further information on the setup of the PI controller are shown in **Appendix B**:(10.3,10.4).
10. Fan	A fan was used to define the mass flow rate in the gas flow cycle(the freezer room), which was defined by changing the input signal from the PI. From the fan, the shaft power of the fan was calculated in order to simulate energy input for the gas flow.

11. Volume — A volume was added to simulate the heat load from the tuna inside the freezer. The volume size was equal to a container (64 m^3). The red heat port shown as an input to the volume is Q flow boundary. It controls the heat load, which was given by a real-input connector, a time table block. Three different heat loads were simulated; 10, 20, and 40 tuna at a length of 2 meters each.

12. COP — A real expression box was used to calculate the coefficient of performance over 24 hours.

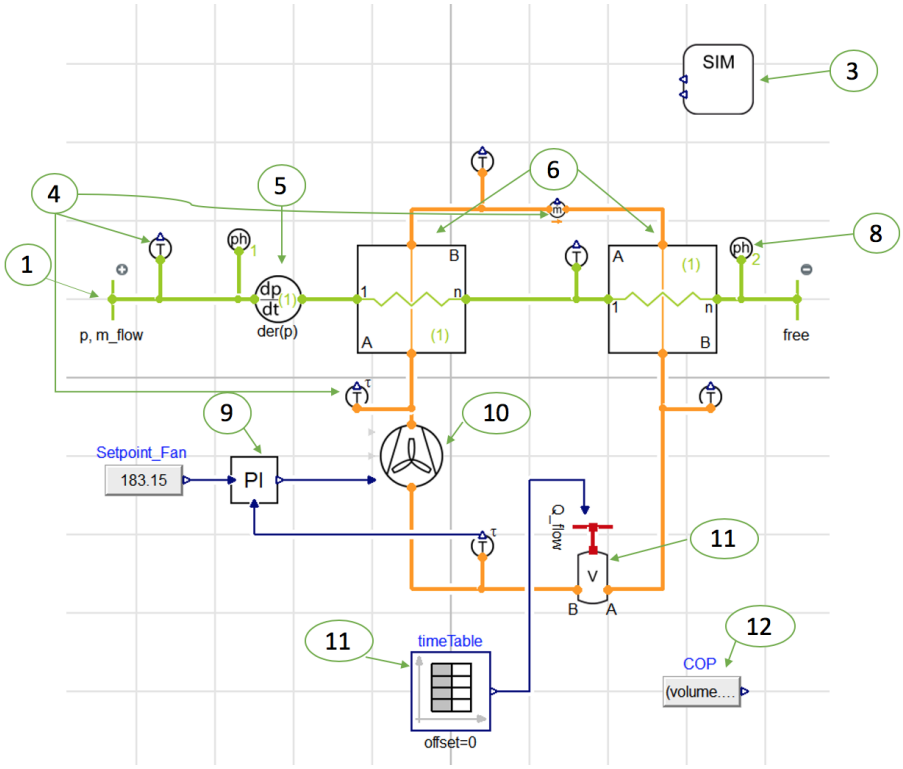

Figure 6.2: Dymola design model of the Direct freezer system for tuna fish freezing

Figure 6.2 shows the model of direct design. A small difference between direct and indirect design. For the direct design, there is one less heat exchanger, and the working fluid in the closed-loop is gone. The VLEfluid (green line) for the direct design is TILMedia_Methane and is now streaming right through the two heat exchangers.

COP was calculated using a real expression (12.COP) calculator in Dymola. For the direct system equation 6.1 was used and for the indirect system equation 6.2 was used.

$$COP = \frac{(volume.heatport.Q\_flow)}{(simpleFan.summary.P\_shaft)} \tag{6.1}$$

$$COP = \frac{(volume.heatport.Q\_flow)}{(simpleFan.summary.P\_shaft + simplePump.P\_drive)} \tag{6.2}$$

Different working fluids were used in the indirect design in Dymola to check how they would behave in terms of COP. The working fluids used in the simulation were TILMediaXTR_Dryair, TILMedia_methane, TILMedia_Nitrogen, Refprop. Air and TILMedia_ethylene. Some of the working fluids used in Dymola was not predefined. They had to be collected from another library in Dymola. For example, was TILMediaXTR_Dryair added and it was done according to this description under: First, the TILMedia menu was opened, and under the VLEFluidTypes menu, a suitable substance was chosen to be duplicate (e.g." TILMedia.CO2"). To assign TILMediaXTR_Dryair as the new property, the vleFluidNames parameter in 6.3 had to be changed to the new name (TILMediaXTR.Dryair).

```
record TILMediaXTR_DryAir "TILMediaXTR.DRYAIR    "
  extends TILMedia.GasTypes.BaseGas(
    final fixedMixingRatio=false,
    final nc_propertyCalculation=1,
    final gasNames={""},
    final concatGasName="TILMediaXTR.DRYAIR",
    final mixingRatio_propertyCalculation={1},
    final condensingIndex=0);

end TILMediaXTR_DryAir;
```

Figure 6.3: Modelica code for a substance in Dymola (TilmediaXTR_DryAir)

Preliminary calculations for the heat exchangers and initialization

For the simulation to run properly in Dymola, the model was build up piece by piece. After adding one heat exchanger, some preliminary calculations for the heat flow, mass flow, pressure, and temperature levels were done in the heat exchanger. The equations used were:

$$Q = \dot{m} C_p \Delta T \tag{6.3}$$

$$\alpha_A = \frac{Q}{\Delta T} \tag{6.4}$$

The values assumed for the VLEFluid was then Δ T = 10 °C, Q = 20kW and C_p = 1.014 $\frac{kJ}{kgK}$. For the gas flow it was assumed Δ T = 6 °C, Q = 20kW and C_p=1.014 $\frac{kJ}{kgK}$. When the model worked properly correct values could be added. For the temperature to in the freezer to be -90°C, the initialization conditions of each heat exchanger and the volume was set to -220°C.

Chapter 7

Results

In this chapter, calculated and simulated results will be presented.

7.1 Thermophysical values

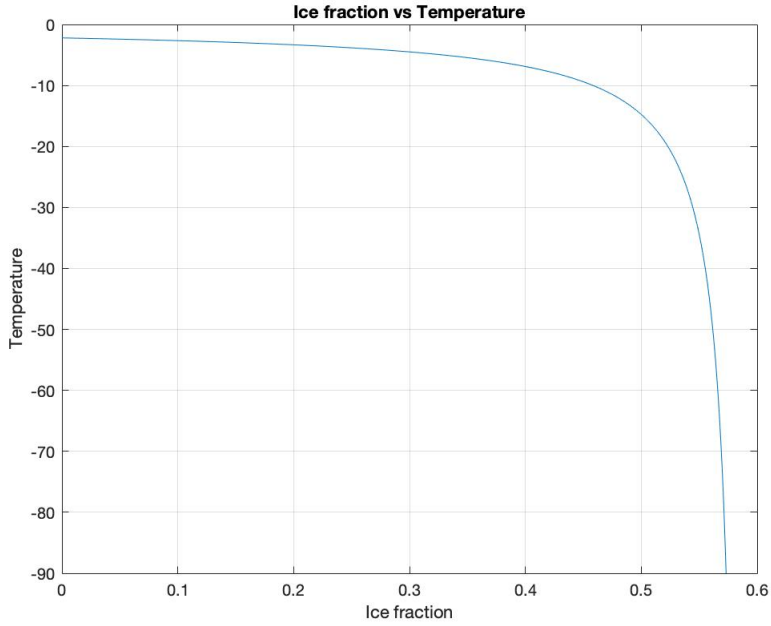

Figure 7.1: Ice fraction as a function of temperature

The ice fraction is dependent on temperature and increases as the temperature decreases, which is seen in figure 7.1. The water is bound to solids in the Tuna, forming solutes at a temperature below freezing point. When the temperature drops, more water transforms into ice crystals, and the solutes become more concentrated. The water content of the Tuna fish above the freezing point is 68%. When the temperature decreases to glass temperature at approximate -72°C, all the water transforms into solid.

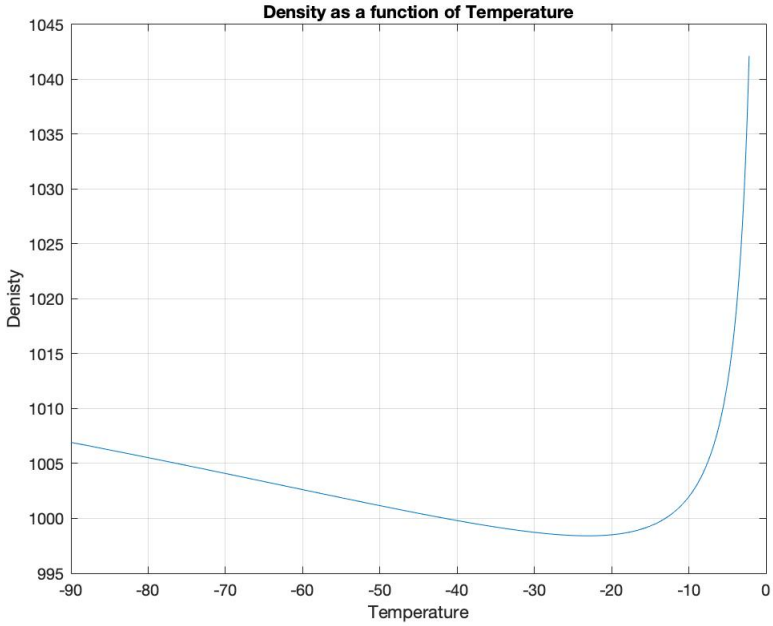

Figure 7.2: Density as a function of temperature

Water has a density of 999.85 kg/m^3 at a temperature of 0.1$°C$, where ice has a density of 916.2 $°C$ at a temperature of 0 $°C$ (EngineeringToolBox, 2003b,a). Because ice has a lower density than water, the density of the tuna will decrease as ice crystals are formed. The most significant density change occurs lower than -10$°C$ (see figure 7.2) due to the high amount of ice crystal formation in the same interval.

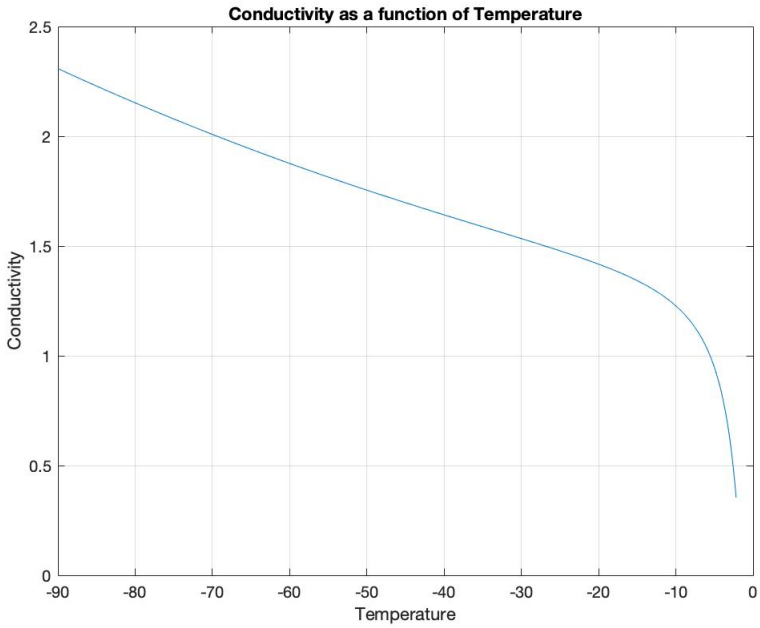

Figure 7.3: Conductivity as a function of temperature

From figure 7.3, it is possible to see that the conductivity is low during the beginning of the freezing. As water transforms into ice crystals, the conductivity increases. Since a large portion of the ice crystals is formed between -2.2$°C$ and -10$°C$ 7.1, the most significant changes of conductivity also exists in this interval.

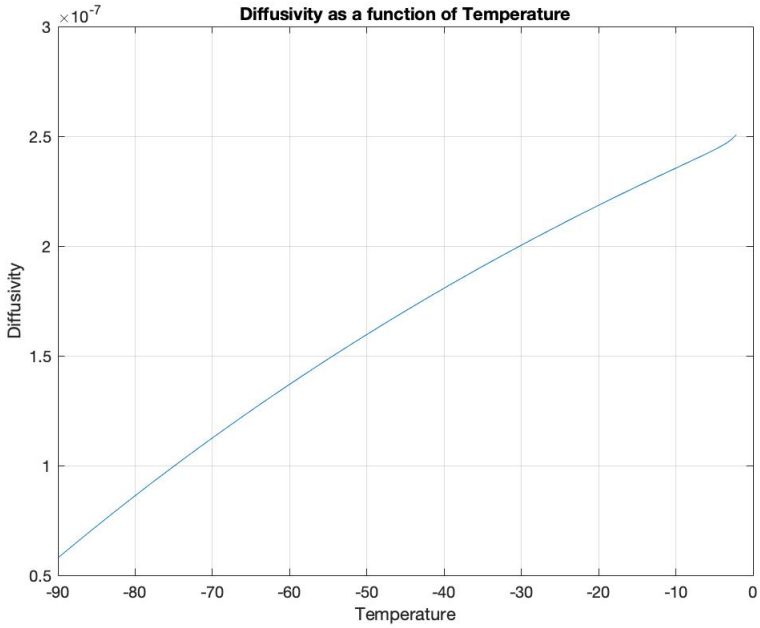

Figure 7.4: Diffustivity as a function of temperature

The diffusivity is a function of conductivity, density and specific heat capacity.

7.2 Tuna model simulation

The tuna model is simulated in Matlab, and the geometry is described in 4.4. The freezer temperature is set to -90°C, and the tuna fish enters the freezer at a freezing point of -2.2°C. Polar coordinates describe the mesh of the tuna, and the heat equation is solved using the FTCS scheme. The diffusivity value of each node is decided according to its temperature. Close to the center of the fish, inaccurate heat transfer in angular direction occurs because the solution diverged if the correct equation were calculated. This is illustrated in figure 7.7.

Four different tuna sized fish has been simulated, three of which are assumed to be frequently caught when fishing. The last size is the largest size a tuna fish can reach. The length of each fish is shown in table 7.1 with corresponding age and weight. Core temperature and freezing effects are calculated with respect to time. Figure 7.7 and 7.8 display the the temperature distribution of cross-section, with perspective from the side (the top of the figure represent the top fin of the fish).

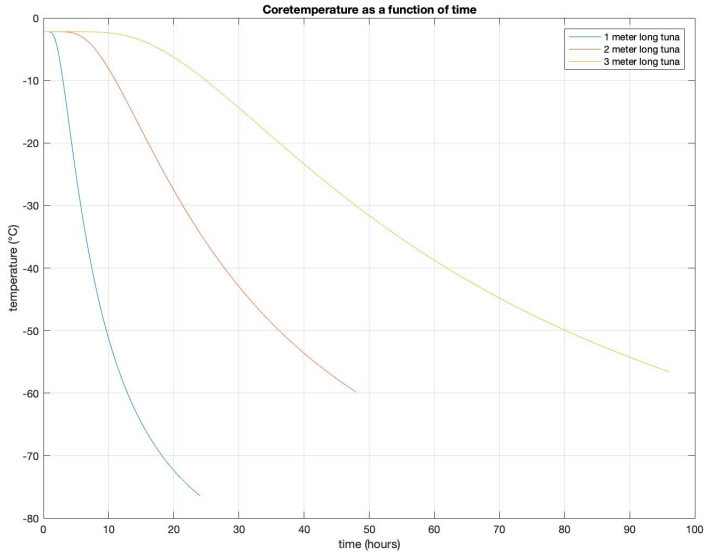

Figure 7.5: The core temperature of three different sized tuna fish. As the diagram display, the freezing time is highly depended on tuna size.

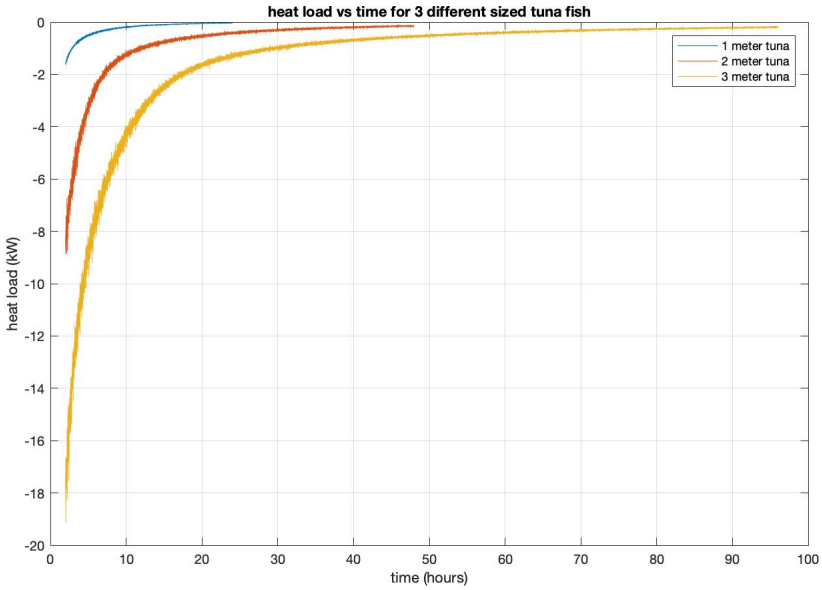

Figure 7.6: The heat load of 3 different sized tuna fish. Notice that the curves starts from 2 hours. This is done to scale the diagram to illustrate the difference between each fish.

	1 meter	2 meter	3 meter
Calculated mass in MATLAB simulation	30 kg	130 kg	321 kg
Actual mass (empirical data)	30 kg	153 kg	520 kg
Deviation	0 %	15 %	38 %

Table 7.1: A comparison between the mass of the different sized tuna (1-, 2- and 3 meters) to the empirical sized tuna. As illustrated, the mass is correct for the 1 meter long tuna, but the tuna at 2- and 3 meters should have been larger compared to the empirical data.

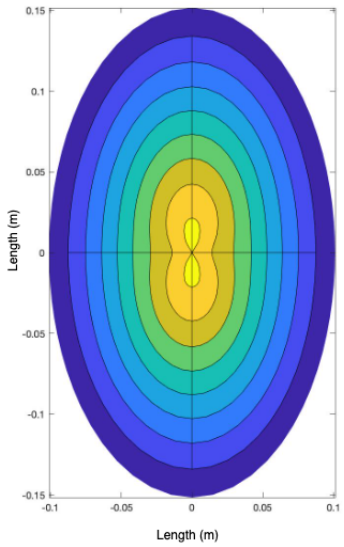

Figure 7.7: Temperature distribution of a cross section of a three meter long Tuna, seen from the front. The yellow colour represents higher temperature than the blue. The distribution is not correct to reality, the reason is elaborated in the next chapter.

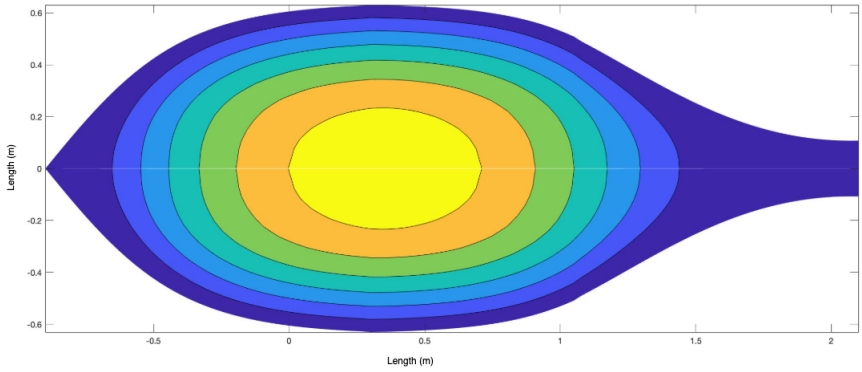

Figure 7.8: Temperature distribution of a cross section of a three meter long Tuna, seen from the side. The yellow colour represents higher temperature than the blue.

7.3 Dymola simulation

The simulation of the freezer designs, both direct and indirect, was done in Dymola. For all the simulations, the temperature was set -90°C in the freezer room. Methane is used to simulate LNG and has a temperature of -162 °C inlet to the freezer designs. Furthermore, to simulate the heat load coming from the tuna in the freezer, the red heat load graph is shown in figure 7.6 was used. This heat load only simulates for one tuna, so in order to get results from having more than one tuna, the red graph was multiplied by 10, 20, and 40. Hence simulations of 10, 20, and 40 tuna in the freezer are used for both direct and indirect design.

7.3.1 Direct design

The direct design uses the LNG cold direct through the heat exchanger and into the batch freezing room. Thus a lower temperature is achievable with a low mass flow of LNG even when there is 40 tuna in the freezer. In figure 7.9 the graphs show how the freezer is behaving during freezing. The red graph with 40 tuna in the freezer increase above 26 °C, this can be seen as irrelevant. The temperature should not increase more than to -2.2 °C since that is the input temperature of the tuna.

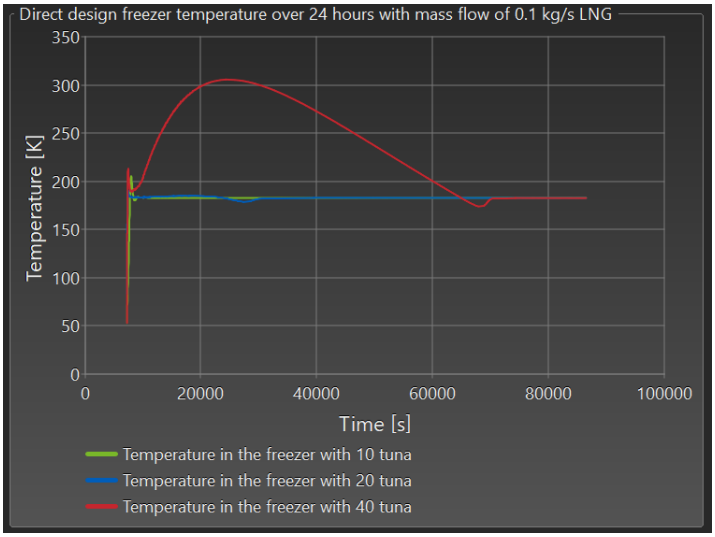

Figure 7.9: Direct system freezer temperature over 24 hours with mass flow of 0,1 kg/s LNG.

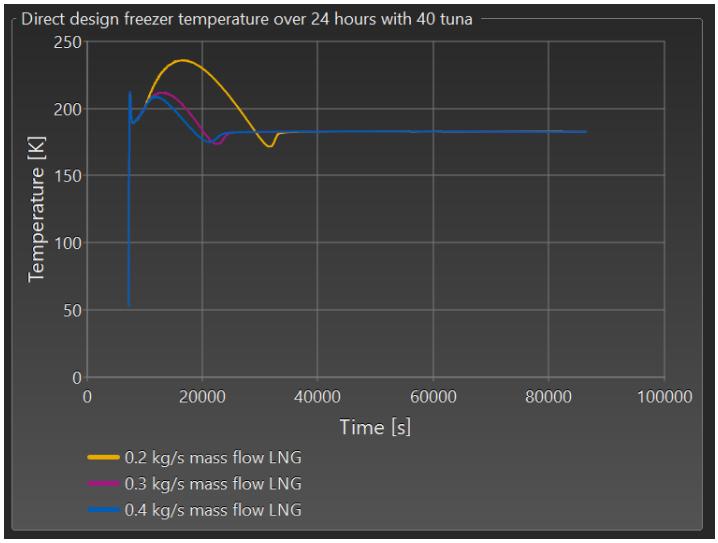

Figure 7.10: Direct system freezer temperature over 24 hours with 40 tuna in the freezer.

From figure 7.9, the low mass flow of LNG at 0.1 kg/s was not sufficient enough to handle the heat load of 40 tuna in the freezer. Hence there should be a higher mass flow of LNG to overcome the heat load, which from figure 7.10 is shown. There are some fluctuations in the start due to the use of a PI regulator for optimizing the mass flow rate in the freezer room. Furthermore, the blue curve reaches the correct temperature of -90 °C first and has a mass flow LNG of 0.4 kg/s. By using a high LNG mass flow, the temperature wanted is reached quickly and without to high increase in the temperature of the freezer. All though the yellow graph in figure 7.10 does not reach a temperature higher than -43.15 °C.

Δh (LNG) [kJ/kg]	Mass Flow LNG [kg/s]	COP (Avg)	Number of tuna
49,088	0,1	15,270	10
98,664	0,1	8,069	20
302,5915	0,1	13,036	40
24,434	0,2	26,667	10
48,298	0,2	24,019	20
96,2465	0,2	19,353	40
16,198	0,3	28,779	10
32,115	0,3	27,136	20
64,0255	0,3	24,067	40
12,139	0,4	29,444	10
24,076	0,4	28,001	20
47,9145	0,4	25,300	40
4,829	1	29,913	10
9,596	1	28,417	20
19,1035	1	25,601	40

Table 7.2: The average COP when freezing 10,20 and 40 tuna in the container at the same time for different mass flow of LNG

From figure 7.2, the average COP values achievable at different amount of LNG in kg/s is shown for a different amount of tuna in the freezer. Furthermore, the enthalpy in and out for the LNG is shown as delta enthalpy, and all of the values are within the two-phase region. The COP values with the highest numbers are marked with a red box around. The most significant increase in COP values happens when increasing from 0.1 to 0.2 kg/s of LNG.

7.3.2 Indirect design

In figure 7.11, the temperature change over 24 hours is shown with a constant mass flow of LNG at 0.3 kg/s. Furthermore, it shows how increasing the heat load increases fluctuation. For a freezer with 40 tuna, it takes more than 13 hours to get the temperature to -90°C, while as for a freezer with ten tuna, it almost immediately stables at -90 °C. In the direct design graph, there were problems with high heat load and low mass flow of LNG, which occur to happen for the indirect design as well.

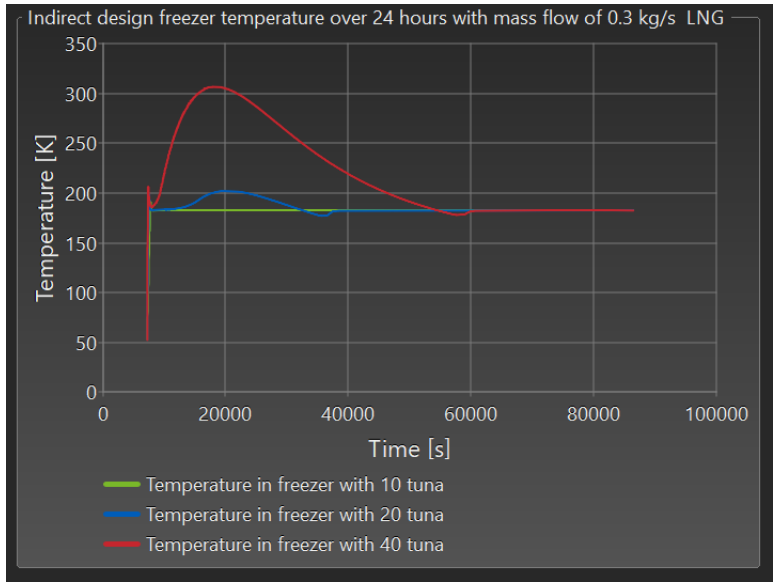

Figure 7.11: Indirect design freezer temperature over 24 hours with 0,3 kg/s mass flow of LNG

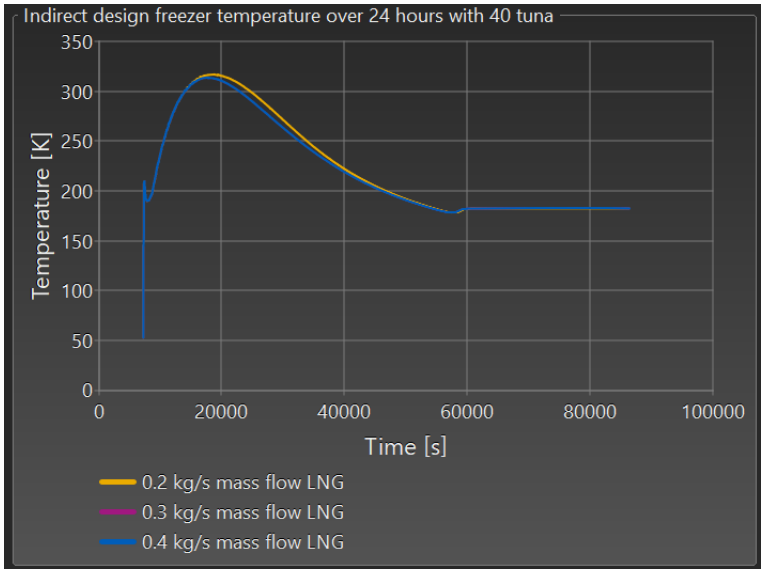

Figure 7.12: Indirect design freezer temperature over 24 hours with 40 tuna and different LNG mass flow

From figure 7.12, an almost identical graph is shown for three different mass flows of LNG. The small amount of increase in mass flow does not seem to decrease the fluctuations for a heat load similar to 40 tuna. It takes a longer time for the freezer temperature to converge to -90°C and it goes over -2.2 °C, which is the initial temperature of the tuna.

Δh (LNG) [kJ/kg]	Mass Flow(LNG) [kg/s]	COP	Mass flow(air) [kg/s]	Number of Tuna	Temperature in closed loop [°C]
27,712	0,2	17,915	5	10	-156,425
57,154	0,2	13,443	5	20	-151,095
143,822	0,2	4,761	5	40	-135,516
55,267	0,2	17,586	10	10	-155,688
57,582	0,2	10,537	10	20	-150,55
139,074	0,2	5,070	10	40	-135,205
55,277	0,2	17,576	15	10	-155,789
83,213	0,2	4,405	15	20	-145,538
137,916	0,2	5,159	15	40	-135,028
18,480	0,3	17,950	5	10	-156,410
37,931	0,3	11,652	5	20	-151,076
94,165	0,3	4,881	5	40	-135,866
18,383	0,3	18,314	10	10	-156,213
37,626	0,3	11,652	10	20	-150,696
91,328	0,3	5,179	10	40	-135,518
18,353	0,3	18,423	15	10	-156,145
37,541	0,3	11,766	15	20	-150,563
90,624	0,3	5,260	15	40	-135,339
13,864	0,4	17,950	5	10	-156,413
28,440	0,4	11,366	5	20	-151,095
70,695	0,4	4,858	5	40	-135,874
13,793	0,4	18,314	10	10	-156,218
28,211	0,4	11,767	10	20	-150,708
68,449	0,4	5,171	10	40	-135,532
13,771	0,4	18,423	15	10	-156,151
28,154	0,4	11,885	15	20	-150,569
67,893	0,4	5,263	15	40	-135,352

Table 7.3: COP of different mass flow for LNG with 10,20 and 40 tuna in the container

This table 7.3 shows the COP values for the indirect design at different mass flow (LNG), mass flow (air), and the number of tuna. Mass flow (air) is for the closed-loop. Furthermore, COP values decrease with an increase in the amount of tuna put in the freezer, and the temperature decreases as the number of tuna increases. All COP values with the red square around are to show the highest COP values achieved with the simulated mass flows.

7.3.3 Choice of refrigerant

	mass flow (LNG) [kg/s]	mass flow (refrigerant) [kg/s]	COP	Number of Tuna
Air	0,1	5	17,469	10
Ethylene	0,1	5	18,093	10
Nitrogen	0,1	5	17,489	10
Methane	0,1	5	17,898	10
Air	0,1	10	17,833	10
Ethylene	0,1	10	18,093	10
Nitrogen	0,1	10	17,840	10
Methane	0,1	10	18,039	10
Air	0,1	15	17,944	10
Ethylene	0,1	15	18,093	10
Nitrogen	0,1	15	17,947	10
Methane	0,1	15	18,084	10

Figure 7.13: COP of Nitrogen, Air and Ethylene as working fluid at mass flow rate of 20 kg/s and LNG mass flow rate at 0,2 kg/S

Figure 7.13 shows how the COP for three different working fluids is. Ethylene has the highest COP value, followed close by methane, air, and nitrogen. All the refrigerant were only tested with the mass flow of 0,1 kg/s LNG and with the same number of tuna in the freezer.

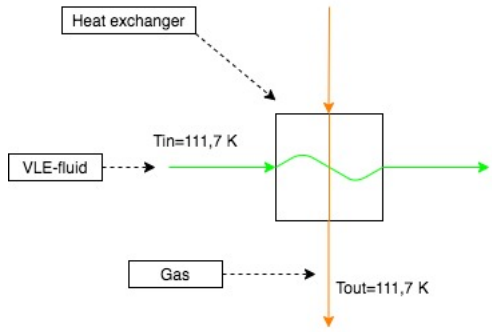

Figure 7.14: The figure shows the temperature difference between two fluids in a heat exchanger before and after the heat exchanger

From this figure 7.14, it is clear that the temperature difference between the two fluids interacting in the heat exchanger is small; it is below 1 K. Hence the heat exchanger is too large. From chapter 3.1 the explanation for this is presented and will be further discussed in the discussion.

Chapter 8

Discussion

The results from the freezer, as well as the tuna model, is based on several assumptions. When simulating a transient model, like the tuna fish model, thermophysical properties change with temperature. As an example, few research papers have investigated the properties of tuna fish below -40$^{\circ}C$, and assumptions have to be made to perform calculations. In this chapter, the assumptions of the different simulation results will be presented. Further, discussions will be made to reach a conclusion of how accurate the results are. Besides that, practical considerations such as fish size, amount of fish, and access to LNG will be discussed.

8.1 Tuna simulation

Thermophysical properties

To describe the temperature variations inside the tuna, thermophysical properties such as density conductivity and specific heat capacity had to be assigned to the tuna. Inside the tuna, the diffusivity describes the rate of heat transfer between each node. Since the diffusivity is dependent on temperature, it has to be updated for each step in time for each node. Below -40$^{\circ}C$, the diffusivity is not valid using the equations from (Kennedy, 2018). Therefore, it was assumed the equations were valid for temperatures as low as -90$^{\circ}C$. It can be argued that the diffusivity not will change significantly since most of the water is transformed into ice crystals at -40$^{\circ}C$. However, the glass transition begins to occur at -55$^{\circ}C$, and does have an impact on the thermophysical properties.

At -40$^{\circ}C$, approximately 80% of the water has transformed into ice crystals. The water will continue to freeze when the temperature is lowered, and at the glass temperature, all of the water will be solidified. The conductivity is highly dependent on the ice fraction, and it is assumed that the conductivity will increase as the temperature decreases. The conductivity is assumed to be valid too -90$^{\circ}C$, using equations from (Kennedy, 2018).

The same assumption is also applied to the density of the tuna.

Matlab calculations

The tuna model assumes that the freezer temperature is continuously equal to -90$^{\circ}C$. Depending on the efficiency of the freezer, it will probably hold a higher temperature at the beginning of the freezing process as the surface of the tuna is not frozen. To improve the results, the Matlab simulation should have been integrated with Modelica; for each time step, the freezer temperature is updated and fed to the tuna simulation. As a consequence, the correct freezer temperature would be given at each time step. Another assumption regarding the surface heat exchange is the constant effusivity for air and fish. The effusivity describes the heat transfer rate between the surface and the air. This will vary due to different air velocities, which are not taken into account.

Furthermore, it is assumed that the curvature of the fish is proportional in thickness and length. By assuming this, it is possible to scale the fish to different sizes in the model. To test the assumption, a comparison between the length-weight correlation described in (Restrepo et al., 2010) and the length-weight correlation of the simulated tuna has been performed 7.1. These results show that the deviation from the model to the empirical data increases with the length of the fish. Since the empirical data suggest that the fish is larger than the simulated model, the longer freezing time has to be expected in reality.

However, the geometry of the tuna is assumed to be a solid body, as it would have been alive. In real life, the tuna is gutted after capture, leaving an open space in the fish where its intestines were. During freezing, the air circulates in this space, lowering the temperature from within the fish. This effect decreases the freezing time significantly.

A weakness of the model is the lack of heat transfer from an angular direction close to the centerline of the tuna. This results in a wrong description of the temperature distribution throughout the fish illustrated in figure 7.7. The reason for this error is the product of $1/R^2$, where R is the distance from the center to the node in the heat equation. When R $-> 0$, the product reaches high values, and the contribution from this factor results in a divergence in the solution. The angular heat transfer is, therefore, only applied halfway to the center. Efforts were made to correct the error. One solution was to split the time interval for nodes close to the center. However, this increases the simulation time significantly, and would not be feasible without powerful computers.

8.2 Dymola simulation

The results from the simulations performed in Dymola describe how different design choices and operational conditions affect the power consumption and the ability to freeze tuna fish. The goal by these simulations is to know the rate of LNG it is necessary to possess to freeze a certain amount of tuna. The results show that the COP value decrease with an increasing amount of tuna. Also, the freezer temperature is not able to hold -90$^{\circ}C$ the first hours of the freezing processes if the heat load is high compared to the LNG flow. The simulation model in Dymola is based on several assumptions listed below. As a consequence of these assumptions, the results are probably not correct, but they can provide guidance to the potential of the freezer. Since the results are based on the same assumptions, they can be compared to each other to find the best solution.

Assumptions

First, the effect in the heat exchangers are assumed to be 2000W/K for the direct design and 333W/K for the indirect design. In addition, frost formation is not included. In reality, frost will accumulate on the heat exchanger in the freezer, causing a thermodynamic resistance. Also, the pressure drop is continuously equal to 2 kPa over the heat exchangers in the freezer for both designs. In a real freezer, the pressure drop will depend on the fan power. Due to a lack of experimental data, the relationship between pressure drop and fan power input is difficult to obtain. Moreover, the heat exchangers are designed to fit the container.

Other findings

From the results of the indirect design, the heat exchanger is approximate ideal 7.14. This implies an over-dimension heat exchanger that would result in high investment costs. The heat exchangers were set to a maximum size to investigate the highest performance. To improve the Dymola model, the heat exchangers should be improved with regards to the heat exchange rate, pressure drop, and size.

The LNG mass flow rates required for sufficient freezing of tuna are fulfilled by all four LNG terminals investigated, assuming that the mass flow is constant throughout the year. Hence, it is feasible to implement the freezer solution at these terminals. The freezer temperature at the beginning of the freezing process is high if the LNG flow is low, in addition to low COP. Therefore, the best alternative would be to install the freezer at the largest terminals, ensuring stable freezing conditions and high COP.

There were two solutions investigated, the indirect and the direct. From the results, the direct design is the preferred method due to high COP and low LNG mass flow consumption for the same freezing conditions. In all the simulations, LNG exits at a liquid/gas state. For the direct design, the temperature of the refrigerant (LNG) is therefore constant at -162$^{\circ}C$. This provides an excellent cold sink for the air in the freezer. On the other hand, the indirect cycle will not provide a refrigerant at such low temperatures. Also, the indirect cycle has more equipment and requires more electricity for the same freezing load. The possible benefit of an indirect freezer is the reduced ice formation due to the

higher temperature of the refrigerant compared to the direct design. The direct method is, therefore, the preferred design.

Chapter 9

Conclusion

The goal of this thesis was to develop a freezer that utilizes the freezing potential from LNG to process tuna fish. The tuna fish marked in Norway started with small fish quotas in 2014, which has increased every year. Due to the relative new tuna quotas, correct processing methods with corresponding infrastructure and market relations are not established. Because of this, the tuna caught in Norway are sold for less than the potential value.

Investigations of tuna have concluded that when frozen to approximate -72$^{\circ}C$, the glass state is reached. The glass state preserves the quality to a much higher degree than conventional freezing at - 24$^{\circ}C$. Consequently, the freezer must hold a temperature lower than the glass temperature. Utilizing LNG as a cold sink for the freezer enables ultra-low freezer temperatures. However, this limits the freezer operation and location to the LNG terminal. Luckily, several LNG terminals are located along the coast of Norway, and all of the investigated LNG terminals has the size of providing sufficient LNG flow for the freezer operation. Fishing boats can unload tuna directly to the terminal of which the freezer is located, decreasing the time from capture to freezing.

Furthermore, the general freezer design was decided from several practical considerations such as mobility, size, ice formation problem, and implementation of existing infrastructure. An insulated container with a fan and a heat exchanger connected to the LNG flow was proposed. Two different heat exchange methods were further investigated in the container design. The direct heat exchange design provided the best results. Additionally, the specific freezer design and operational conditions were investigated using simulation tools. Due to the lack of empirical data, several assumptions such as tuna size and pressure drop in the freezer were made. These assumptions weaken the legitimacy of the numerical results. However, the results provide a comparison basis for different designs and operations conditions.

The results displayed that there were significant variations of freezing time with different sized tuna fish at freezing temperatures of -90$^{\circ}C$. Reaching a core temperature of

-60°C took approximately 13 hours for a 1 meter long tuna, compared to 2 days for a 2 meter- and over four days for a 3 meter long tuna. However, the fish was simulated as a solid body, without being gutted, that will affect the freezing time significantly. Results from the direct heat exchange design, a mean COP value between 8 and 30, were derived. The low COP values occurred when there was low LNG mass flow compared to the freezer heat load. The high COP values occurred in the opposite situation when there was an excess of LNG flow compared to the freezer heat load.

The proposed freezer solution is superior to excising technology due to the high COP. It is simple to integrate the freezer to an existing LNG terminal, and the freezer is not expensive. In addition, the freezer can freeze tuna fish to ultra-low temperatures. Implementation of this freezer would, however, demand a market connection to Japan. A trustworthy market system must be established to be able to extract the potential value of the tuna fish. Therefore, a proposed tag system can be applied to grade each fish according to quality and processing details. This will provide the wholesaler in Norway, the buyer in Japan, and other actors a trustworthy business platform.

Chapter 10

Further work

This thesis has laid a basis for which further investigations can be carried out. Several freezing techniques have been explored, as well as theoretical aspects of ultra-low temperature fish freezing. The proposed solution can be further investigated with experiments, improving the results from this thesis. Besides, marked relations should be elaborated to understand if the solution can be commercialized.

The simulations in this thesis are based on models with several assumptions. It is not elaborated on the error margin these assumptions case to the results. In further work, the models should be improved to eliminate the margin of error and to generate more realistic results. Also, the tuna heat distribution function should be integrated as a part of the freezer simulation in order for the models to communicate.

In order to get a better understanding of the thermophysical properties of a tuna during a freezing, and the operational conditions of a freezer utilizing LNG, experiments should be performed. The data from these experiments should improve the boundary conditions and input parameters for the simulations. The model can then be improved and be more reliable if an LNG freezer is going to be designed. Experimental data can also discover unforeseen events that are not taken into account in the current models.

Furthermore, improved market insight is essential to develop a business model for tuna freezing utilizing LNG. Both fishing- and LNG companies should be contacted to establish cooperation between the two. Such a study would lead to a better understanding of the economics and what the profit of a tuna freezer potential can gain. In addition, connections to the marked in Japan should be initiated to provide a better understanding of the tuna quality demands as well as business connections.

Bibliography

Åström, K.J., Hägglund, T., 1995. *PID controllers: theory, design, and tuning*. Instrument society of America Research Triangle Park, NC.

Augustini, T.W., Suzuki, T., Hagiwara, T., Ishizaki, S., Tanaka, M., Takai, R., 2001. Change of k value and water state of yellowfin tuna thunnus albacares meat stored in a wide temperature range (20°c to -84°c). *Fisheries science,* 67, 306–313.

Bhandari, B., Howes, T., 1999. Implication of glass transition for the drying and stability of dried foods. *Journal of Food Engineering,* 40, 71 – 79.

Boonsumrej, S., Chaiwanichsiri, S., Tantratian, S., Suzuki, T., Takai, R., 2007. Effects of freezing and thawing on the quality changes of tiger shrimp (penaeus monodon) frozen by air-blast and cryogenic freezing. *Journal of Food Engineering,* 80, 292–299.

Carroll, M.T., Anderson, J.L., Martínez-Garmendia, J., . Pricing u.s. north atlantic bluefin tuna and implications for management. *Agribusiness,* 17, 243–254.

Çengel, Y.A., 2020. Power generation potential of liquified natural gas regasification terminals. *International Journal of Energy Research,* 44, 3241–3252.

Chandra, V., 2020. *What is Natural Gas?* Available at: http://www.natgas.info/gas-information/what-is-natural-gas. (accessed 29-May-2020).

Chen, C.S., 1985. Thermodynamic analysis of the freezing and thawing of foods, enthalpy and apparent specific heat. *Journal of Food Science,* 50, 1158–1162.

Crigler, J., Dawson, L., 1968. Cell disruption in broiler breast muscle related to freezing time. *Journal of Food Science,* 33, 248–250.

Dempsey, P., Bansal, P., 2012. The art of air blast freezing: Design and efficiency considerations. *Applied Thermal Engineering,* 41, 71–83.

Egashira, S., 2013. Lng vaporizer for lng re-gasification terminal. *KOBELCO Technology Review,* 32, 64–69.

Eikvik, T.M., 2020. One stage vapor compression cycle. *TEP4255 Heat Pumping Processes and Systems* Available at: https://ntnu.blackboard.com (accessed 3 February 2020.

EngineeringToolBox, 2003a. *Ice - Thermal Properties*. Available at: https://www.engineeringtoolbox.com/ice-thermal-properties-d_576.html (accessed 10 April 2020).

EngineeringToolBox, 2003b. *Water - Density, Specific Weight and Thermal Expansion Coefficient*. Available at: https://www.engineeringtoolbox.com/water-density-specific-weight-d_55.html (accessed 10 April 2020).

Fellow, P.J., 2000. Food Processing Technology - Principles and Practice (2nd Edition). Woodhead Publishing.

Fiskeridirektoratet, 2019. *Fiske etter makrellstørje i 2019*. Avaliable at: https://www.fiskeridir.no/Yrkesfiske/Tema/Makrellstoerje (accessed 17 February 2020).

Foss, M.M., Head, C., 2007. Introduction to lng. Center For Energy Economics, Available at: http://www. beg. utexas. edu/energyecon/lng/documents/CEE_INTRODUCTION_TO_LNG_FINAL. pdf (accessed 5 March 2020) 11, 2011.

Gavelli, F., 2010. *Computational fluid dynamics simulation of fog clouds due to ambient air vaporizers*. Journal of Loss Prevention in the Process Industries 23, 773–780.

Goswami, T.K., 2001. *Cryogenic fish freezing: Science, Technology & Economics*. Available at: https://me.buet.ac.bd/icme/icme2001/cdfiles/Papers/Thermal/32_final_TE-09(179-184).pdf. (accessed 15 February 2020).

Inoue, C., Ishikawa, M., 1997. Glass Transition of Tuna Flesh at Low Temperature and Effects of Salt and Moisture. *Journal of Food Science* 62, 496–499.

Jensen, K.N., Jørgensen, B.M., Nielsen, J., 2003. Low-temperature transitions in cod and tuna determined by differential scanning calorimetry. *LWT - Food Science and Technology* 36, 369 – 374.

Johnston, W., 1994. Freezing and refrigerated storage in fisheries. volume 340. Food & Agriculture Org.

Karel, M., Fennema, O.R., Lund, D.B., 1975. Principles of food science. Part II. Physical principles of food preservation. Marcel Dekker, Inc., New York, USA.

Kennedy, H.E. (Ed.), 2018. Ashrae handbook refrigeration. American Society of Heating, Refrigerating and Air Conditioning Engineers.

Lakshmisha, I., Ravishankar, C., Ninan, G., Mohan, C.O., Gopal, T., 2008. Effect of freezing time on the quality of indian mackerel (rastrelliger kanagurta) during frozen storage. Journal of food science 73, S345–S353.

Love, R., 1958. The expressible fluid of fish fillets. viii.—cell damage in slow freezing. Journal of the Science of Food and Agriculture 9, 257–262.

Mallett, C.P., 1993. Frozen food technology. Springer Science & Business Media.

Mathworks, . Avaliable at: https://www.mathworks.com/discovery/what-is-matlab.html (accessed 25 March 2020).

Orlien, V., Risbo, J., Andersen, M.L., Skibsted, L.H., 2003. The question of high-or low-temperature glass transition in frozen fish. construction of the supplemented state diagram for tuna muscle by differential scanning calorimetry. *Journal of agricultural and food chemistry,* 51, 211–217.

Ottolenghi, F., 2008a. Capture-based aquaculture of bluefin tuna. *Capture-based aquaculture. Global overview. FAO Fisheries technical Paper,* 508, 169–182.

Ottolenghi, F., 2008b. Capture-based aquaculture of bluefin tuna. Capture-based aquaculture. Global overview. FAO Fisheries technical Paper 508, 169–182.

Patel, D., Mak, J., Rivera, D., Angtuaco, J., 2013. Lng vaporizer selection based on site ambient conditions. *Proceedings of the LNG,* 17, 16–19.

Restrepo, V., Diaz, G., Walter, J., Neilson, J., Campana, S., Secor, D., Wingate, R., 2010. Updated estimate of the growth curve of western atlantic bluefin tuna. *Aquatic Living Resources,* 23, 335 – 342.

Roos, Y.H., 2010. Glass transition temperature and its relevance in food processing. *Annual Review of Food Science and Technology,* 1, 469–496.

Roul, M., Tripathy, S., Jena, J., Padhiary, D., 2014. Thermodynamic analysis of a cascade refrigeration system based on carbon dioxide and ammonia. *Journal of Engineering Research and Applications,* Vol. 4.

Statistisksentralbyrå, 2020. *Produksjon og forbruk av energi, energibalanse*. Avaliable at: https://www.ssb.no/energi-og-industri/statistikker/energibalanse (accessed 17 February 2020).

Streit, J., Razani, A., 2013. Thermodynamic optimization of reverse brayton cycles of different configurations for cryogenic applications. *International journal of refrigeration,* 36, 1529–1544.

Sun, D.W., 2016. Handbook of frozen food processing and packaging. CRC press.

Tan, F.L., Fok, S.C., 2009. Freezing of tilapia fillets in an air blast freezer. *International Journal of Food Science & Technology,* 44, 1619–1625.

Tolstorebrov, I., 2019. conversation.

Valencia-Perez, A.Z., Soto-Valdez, H., Ezquerra-Brauer, J.M., Márquez-Ríos, E., Torres-Arreola, W., 2015. Quality changes during frozen storage of blue shrimp (litopenaeus stylirostris) with antioxidant, α-tocopherol, under different conditions. *Food Science and Technology,* 35, 368–374.

Valentas, K.J., Rotstein, E., Singh, R.P., 1997. *Handbook of food engineering practice*. CRC press.

Widell, K.N., 2020. Private Communication.

Wlodek, T., 2019. Analysis of boil-off rate problem in liquefied natural gas (lng) receiving terminals. *IOP Conference Series: Earth and Environmental Science,* 214, 012105.

Woll, T., Svendgård, O., 2015. Norskekysten lng utvikling av infrastruktur for lng som drivstoff i norge. Available at: https://docplayer.me/16709434-Norskekysten-lng-utvikling-av-infrastruktur-for-lng-som-drivstoff-i-norge.html (accessed 14 February 2020.

Xin ZhiQiang, W.C., 2013. Shape optimization of the caudal fin of the three-dimensional self-propelled swimming fish. *Science China Physics, Mechanics and Astronomy,* .

Yılmaz, F., Selbaş, R., Özgür, A.E., Balta, M.T., 2016. Performance analyses of co 2-n 2 o cascade system for cooling. *Energy, Transportation and Global Warming,* , 499–512.

Ziegler, F., Winther, U., Hognes, E.S., Emanuelsson, A., Sund, V., Ellingsen, H., 2013. The carbon footprint of norwegian seafood products on the global seafood market. *Journal of Industrial Ecology,* 17, 103–116.

Appendix

10.1 Appendix A - Parameters for Heat Exchanger in Dymola

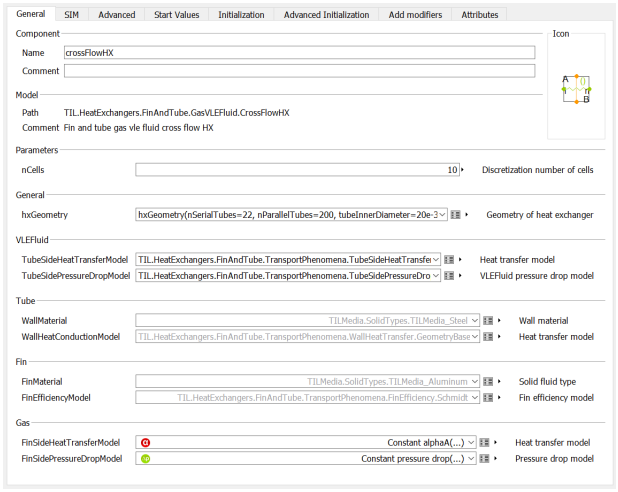

Figure 10.1: Heat exchanger values in Dymola

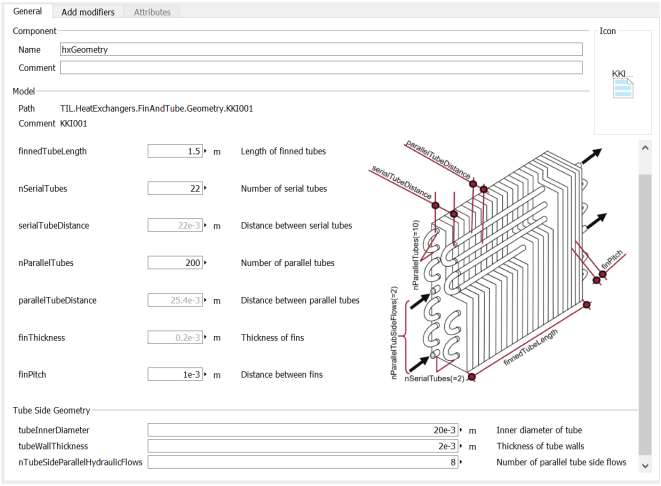

Figure 10.2: Heat exchanger geometry in Dymola

10.2 Appendix B - Parameters for PI controller in Dymola

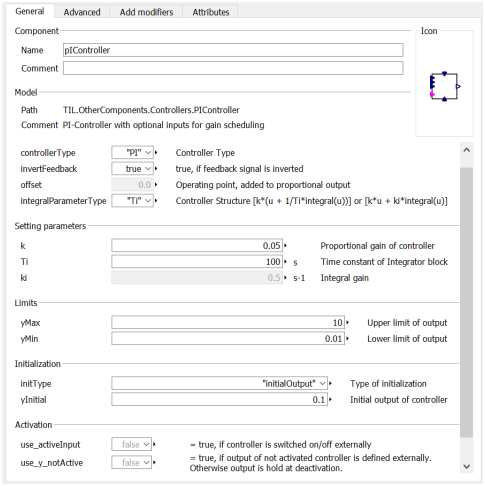

Figure 10.3: PI controller in Dymola

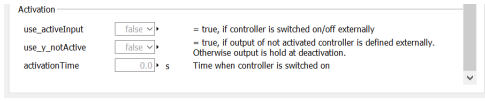

Figure 10.4: PI controller in Dymola

10.3 Appendix C - Parameters for preliminary calculations used in Dymola for the heat exchanger

	VLEFluid initial	Gas initial
Mass flow [kg/s]	−1,9724	3,28
Alpha [W/K]	2000	3333
T (før HX) [◦C]	−120	−110
T (etter HX) [◦C]	−69	−75
ΔP [Pa]	0	0

Figure 10.5: Preliminary calculation results for the heat exchanger

10.4 Appendix D - Matlab code calculating the thermal properties of a tuna in a freezing process

10.4.1 Function calculating the temperature distribution within the tuna fish

```
function ans = tunaHeat

%effusivity
cond_air = 16.2*10^-3;
rho_air = 1.75;
cp_air = 1;
eFreezer = sqrt(cond_air*rho_air*cp_air);

%enthalpy values
enthalpyfunk = deltaH;
h = enthalpyfunk(:,1).' ;
htemp = enthalpyfunk(:,2).'*10;
htemp = int16(htemp);

%thermophysical values
thermovalues = ThermoProp;
rho_values = thermovalues(:,1).';
alpha_values = thermovalues(:,2).';
effusivity = thermovalues(:,3);

% Geometry descritization
dx = 0.03; %distance between each cross section
dtheta = pi/(2*12); %number of js

Lx = 2*[-0.3:dx:0.7]; %x-values of fish.
theta = -dtheta:dtheta:pi/2; %theta-values
nx = length(Lx); %number of x-values

nr = 16; % # steps in radial direction

% Time values
dt = 2;%timestep
hours = 24; % numers of hour simulation
Nt = 3600*1/dt*hours;%number of timesteps

% Initial condition
t=0;
FreezerTemp = -90;

%Set initial conditions to -2.2°C for the fish
for i = 1:length(Lx) %Runs through each cross section in x-direction
   for j = 1:length(theta)
        for  r = 1:nr
             Tn(i,j,r) = -2.2;
        end
   end %theta
end %x


%Set bondary condition for maximum radial values (surface of tuna)
for i = 1:length(Lx) %Runs through each cross section in x-direction
 and set surfa
```

```
   for j = 1:length(theta)
        Tn(i,j,nr) = FreezerTemp;
   end %theta
end %x

%Set boundary condition for the tip and the tail of the fish to -80°C
for i = 1:length(Lx)-1:length(Lx)
   for j = 1:length(theta)
        for  r = 1:nr % the edge of the ellipse
             Tn(i,j,r) = FreezerTemp;
        end
   end %theta
end %x

surface = Surface(dx,dtheta,nr); %extracts diffusivity parameters for
 each node
dist = distance(dx,dtheta,nr); %extracts values for the distance for
 the given node to the nodes beside

%Calculates new temperature from heat equation at each timestep
for n = 1:Nt
    t = t+dt; % New time
    Tc = Tn; % Save the temperature

    %Updates the boundary conditions at theta = 0 and theta = Pi/2 (or
 90°)
    Tc(:,length(theta)+1,:) = Tn(:,length(theta)-1,:);
    Tc(:,1,:) = Tn(:,3,:);
    cont = cont+1;


  for i = 2:nx-1 %Runs through each cross section in x-direction
      for j = 2:length(theta)
           for  r = 1:nr


               Temp_approx = int16(round(Tn(i,j,r),1)*10); %Find
 temperature with one decimial for the node
               k = find(Temp_approx == htemp);

               alpha_temp = alpha_values(k);   %diffusivity
               eTuna = effusivity(k); %effusivity


               a_out = alpha_temp; %diffustivity state to the node
 one step  the surface (r+1)
               a_left    = alpha_temp; %diffustivity state to the
 left node (i-1)
               a_right  = alpha_temp; %diffustivity state to the
 right node (i+1)

%                   extract distances to the nearby nodes
               ds_left = dist(i,j,r,1); %distance to node i-1
               ds_right= dist(i,j,r,2); %distance to node i+1
```

```
                dr      = dist(i,j,r,3); %radial distance, r+1 or r-1
                R       = dist(i,j,r,4); %distance from center to node
 r


                if r >1 %ignores inner circle
                volume = R*dr*dtheta*(ds_right/2 + ds_left/2);
                rho = rho_values(k);
                enthalpy = h(k);
                enthalpy_node(i,j,r) = enthalpy*rho*volume;

                end
%

                if surface(i,j,r) == true  % if on surface, calculate
 the temperature with effusivity equation

                Tn(i,j,r) = Tc(i,j,r) + (FreezerTemp-
Tc(i,j,r))*(eFreezer/(eFreezer+eTuna));

                else % heat equation

%
                %calculates the enthalpy



                if r == 1  % no heat transfer in theta direction
                Tn(i,j,r) = Tc(i,j,r) + dt*(...
                (Tc(i+1,j,r) - Tc(i,j,r))*a_right/(ds_right)^2  +
 (Tc(i-1,j,r)-Tc(i,j))*a_left/(ds_left)^2+...
                (Tc(i,j,r+1)-Tc(i,j,r))*alpha_temp/(dr/2)^2);%+ ...
                %1/(dr)^2 * (Tc(i,j+1,r)- 2*Tc(i,j,r) +
 Tc(i,j-1,r) )*alpha_temp/(dtheta)^2);

                elseif r <7 %The reason for the split of r is the
 factor 1/R^2 (last line). Since R->0 when r is low, the equation
 diverge when r is low.

                Tn(i,j,r) = Tc(i,j,r) + dt*(...
                (Tc(i+1,j,r) - Tc(i,j,r))*a_right/(ds_right)^2  +
 (Tc(i-1,j,r)-Tc(i,j,r))*a_left/(ds_left)^2 + ...% heat in x-direction
                1/R * ( (R-dr/2)*alpha_temp*Tc(i,j,r-1) - ((R
+dr/2)*a_out+(R-dr/2)*alpha_temp)*Tc(i,j,r) + (R+dr/2)*a_out*Tc(i,j,r
+1))/(dr^2) +... %heat in radial direction
                1/(R*0.1) *(Tc(i,j+1,r)- 2*Tc(i,j,r) +
 Tc(i,j-1,r) )*alpha_temp/(dtheta)^2); %heat in theta direction

                else %
                Tn(i,j,r) = Tc(i,j,r) + dt*(...
                (Tc(i+1,j,r) - Tc(i,j,r))*a_right/(ds_right)^2  +
 (Tc(i-1,j,r)-Tc(i,j,r))*a_left/(ds_left)^2 + ...
```

```
                1/R * ( (R-dr/2)*alpha_temp*Tc(i,j,r-1) - ((R
+dr/2)*a_out+(R-dr/2)*alpha_temp)*Tc(i,j,r) + (R+dr/2)*a_out*Tc(i,j,r
+1))/(dr^2) +...
                1/(R*R)*(Tc(i,j+1,r)- 2*Tc(i,j,r) +
 Tc(i,j-1,r) )*alpha_temp/(dtheta)^2);
                end %if
                end % if surface

            end %r
        end %theta
    end %x

coreTemp(n) = max(max(max(Tn)));

%    updates boundary at theta = 0 and pi/2
   Tn(:,length(theta)+1,:) = Tn(:,length(theta)-1,:);
   Tn(:,1,:) = Tn(:,3,:);

ent(n) = sum(sum(sum(enthalpy_node)));
if n > 1
    effect(n) = ent(n)-ent(n-1);
end


end %time loop

theta(1)=[];


% Prints the temperature distribution at cross sectionsection = x
section = 5;
radius = squeeze(dist(section,:,:,4));
r = radius(1,:);
radius(1,:) = [];
[RADI,THETA] = meshgrid(r,theta);
[x,y]= pol2cart(THETA,radius);
TEMP = Tn(section,:,:);
TEMP = squeeze(TEMP);
x = [x;flip(x)];
x = [x;-flip(x)];
y = [y;-flip(y)];
y = [y;flip(y)];
TEMP = [TEMP;flip(TEMP)];
TEMP = [TEMP;flip(TEMP)];
contourf(x,y,TEMP) % prints cross section at x-section defined in line
 200

%Prints the temperature distribution in cross section seen from the
 side
matrix = squeeze(dist(:,length(theta),:,4));
midler = matrix(1,:);
[Yvalue,Xvalue] = meshgrid(midler,Lx);
Tempv = squeeze(Tn(:,length(theta),:));
Tempv = [Tempv;flip(Tempv)];
```

```
Xvalue = [Xvalue;flip(Xvalue)];
matrix = [matrix;-flip(matrix)];
contourf(Xvalue,matrix,Tempv);

ans = Tn;%Temperature distribution at the end of the simulation

end %function
```

```
Undefined function or variable 'cont'.

Error in tunaHeat (line 77)
    cont = cont+1;
```

Published with MATLAB® R2017b

10.4.2 Function calculating the enthalpy change with temperature

```
function [H,temp]= deltaH
T_freezer = -90;
dT = 0.1;
T_int = -2.2;                   % Initial freezing temperature of Tuna
 fish, °Celsius

T_intK = 273.15+T_int;          % Initial freezing temperature of Tuna
 fish, Kelvin
T_freezerK = 273.15+T_freezer;  % Freezer temperature, Kelvin

x_p = 0.2333;                   % Mass fraction of protein in Tuna
x_wo = 0.6809;                  % Mass fraction of water in the
 unfrozen Tuna
c_u = 3.43;                     % Specific heat capacity of Tuna

x_b = 0.4*x_p;                  % Mass fraction of bound water
Dc_p = 4.18-2.108;              % Difference between specific heat of
 water and ice
x_s = 1-x_wo;                   % Mass fraction of solids

T_0 = 273.15;                   % Freezing temperature of water,
 Kelvin
L_0 = 333.6;                    % Latent heat of Tuna fish, kJ/kg

T_prodK = T_intK:-dT:T_freezerK;    % Vector from initial freezing
 temperature to end of freezing, Kelvin
T_prodC = T_int:-dT:T_freezer;     % Vector from initial freezing
 temperature to end of freezing, Celcius

H = zeros(length(T_prodC),2);


for i = 1:length(T_prodK)

     dH_schw(i) = (T_prodK(i)-T_freezerK)*(c_u + (x_b-x_wo)*Dc_p
 -  ((x_wo-x_b)*L_0*(T_int)) / ((T_0 - T_freezerK) * (T_0 -
 T_prodK(i))));

     %dH_chen(i) = (T_prodC(i)-T_freezer)*(1.55 + 1.25 * x_s-((x_wo-
x_b)*L_0*T_int)/(T_freezer*T_prodC(i)));
     H(i) = dH_schw(i);
     H(i,2) = T_prodC(i);
end


% H(2) = dH_schw;

% plot (T_prodC, dH_schw )


end
```

10.4.3 Function calculating the distance between each node

```
function ans = distance(dx,dtheta,nr)

% Geometry descritization

Lx = -0.3:dx:0.7;
theta = 0-dtheta:dtheta:pi/2;

 % # steps in radial direction

mat = zeros(length(Lx),length(theta),nr,4);

% THe following code calculates the distance between each node in x-
direction both left and right (-ds,ds) as well
% as in radial direction (dr) and the distance from center (R). These
 four
% distances are added as the 4th dimension in matrix mat.

% 1: (i-1) distance to node at left cross section
% 2: (i+1) distance to node at right cross section
% 3: dr: distance to node both in and out (r+1) and (r-1)
% 4: R: distance from center to node

for i= 1:length(Lx) %Runs through each cross section in x-direction

% Calculate a and b value for ellipse function at each cross section.
% Functions given by report.
   if  Lx(i) < 0.1
       a = 0.152*tanh(6*(Lx(i))+1.8);

   elseif Lx(i) >= 0.1 && Lx(i)<0.35
       a = 0.075 - 0.076*tanh(7*Lx(i)-3.15);

   else
       a = 1.749*tanh(Lx(i)) - 3.331*tanh(2*Lx(i)) +
 1.976*tanh(3*Lx(i));
   end

   b = a*1.5;

       for j = 1:length(theta)
            r_max(i,j) = 2*(1/((((cos(theta(j))^2)/
a^2)+((sin(theta(j)))^2/b^2))))^0.5; % Calculates the distance from
 center to the edge og the ellipse
            dr(i,j) = r_max(i,j)/(nr); %calculates the radial step
 for each cross section and angle


            for r = 1:nr
                mat(i,j,r,3) = dr(i,j); %dr

                if i == 1 || i == 2 % avoid the first cross section
```

```
                else
                mat(i-1,j,r,1) = 2*(dx^2 + (  (r_max(i-1,j)-
dr(i-1,j)*(nr-r)) - (r_max(i-2,j)-dr(i-2,j)*(nr-r))  )^2  )^0.5;  % ds
 left cross section (i-1)
                mat(i-1,j,r,2) = mat(i-1,j,r,1);  %(dx^2 + (
  (r_max(i-1,j)-dr(i-1,j)*(nr-1)) - (r_max(i,j)-dr(i,j)*(nr-r))
  )^2  )^0.5; % ds right cross section (i+1)
                end

                if r == 1
                mat(i,j,r,4) = dr(i,j)/50; % impossible to define a
 center. Decreases the distance from center to r=1 to dr/10
                else
                mat(i,j,r,4) = dr(i,j)*(r-1); %caluclates the
 distance from center to r
                end

            end %r
       end %theta
end %x


ans = mat;

end %function
```

```
Not enough input arguments.

Error in distance (line 5)
Lx = -0.3:dx:0.7;
```

Published with MATLAB® R2017b

10.4.4 Function calculating the ice fraction as a function of temperature

```
function ice_fraction = IceFractionOfTemp


dT = 0.1;
T_low_tuna = -90;
T_int = -2.2;                   % Initial freezing temperature of Tuna
 fish, °Celsius

x_p = 0.2333;                   % Mass fraction of protein in Tuna
x_wo = 0.6809;                  % Mass fraction of water in the
 unfrozen Tuna
x_f = 0.049;                    % Mass fraction of fat in Tuna
x_a = 0.0118;                   % Mass fraction of ash in Tuna
x_b = 0.4*x_p;                  % Mass fraction of bound water


T_prod = T_int:-dT:T_low_tuna;     % Vector from initial freezing
 temperature to end of freezing, Celcius


for i = 1:length(T_prod)
    iceF(i) = (x_wo - x_b)*(1-T_int/T_prod(i));     % Miles (1974)
end

ice_fraction = iceF;


end
```

10.4.5 Function calculating the thermal properties as a function of temperature

```
function ans = ThermoProp


dT = 0.1;
T_low_tuna = -90;
T_int = -2.2;            % Initial freezing temperature of Tuna fish,
 °Celsius

x_ice = IceFractionOfTemp;

x_p = 0.2333;                    % Mass fraction of protein in Tuna
x_wo = 0.6809;                   % Mass fraction of water in the
 unfrozen Tuna
x_s = 1-x_wo;                    % Mass fraction of solids
x_f = 0.049;                     % Mass fraction of fat in Tuna
x_a = 0.0118;                    % Mass fraction of ash in Tuna
x_b = 0.4*x_p;                   % Mass fraction of bound water
x_w = x_wo-x_ice;
c_u = 3.43;                      % Specific heat capacity of Tuna

x = x_w+x_ice;

Dc_p = 4.18-2.108;               % Difference between specific heat of
 water and ice
x_s = 1-x_wo;                    % Mass fraction of solids

T_0 = 273.15;                    % Freezing temperature of water,
 Kelvin
L_0 = 333.6;                     % Latent heat of Tuna fish, kJ/kg

T_prod = T_int:-dT:T_low_tuna;     % Vector from initial freezing
 temperature to end of freezing, Celcius

for i = 1:length(T_prod)
    %Density
    rho_w(i) =
 9.9718*100+3.1439*0.001*T_prod(i)-3.7574*0.001*T_prod(i).^2;
    rho_ice(i) = 9.1689*100-0.13071*T_prod(i);
    rho_p(i) = 1.3299*1000-0.5184*T_prod(i);
    rho_f(i) = 925.59-0.41757*T_prod(i);
    rho_a(i) = 242.38-0.28063*T_prod(i);

    mean_rho(i) = 1/(x_ice(i)/rho_ice(i) + x_w(i)/rho_w(i)+ x_p/
rho_p(i) + x_f./rho_f(i) + x_a/rho_a(i));

    %conductivity
    k_w(i) = 0.57109 + 1.7635*0.001*T_prod(i) -
 6.7036*10^(-6)*(T_prod(i))^2;
    k_ice(i) = 2.2196 - 6.2489*0.001*T_prod(i) +
 1.0154*10^(-4)*(T_prod(i))^2;
    k_p(i) = 1.7881*0.1 + 1.1958*10^(-3)*T_prod(i) -
 2.7178*10^(-6)*(T_prod(i))^2;
```

```
    k_f(i) = 1.8071*0.1 - 2.7604*10^(-3)*T_prod(i)
 -1.8849*10^(-7)*(T_prod(i))^2;
    k_a(i) = 3.2962*0.1 + 1.4011*10^(-3)*T_prod(i) -
 2.9069*10^(-6)*(T_prod(i))^2;

    %diffusivity
    a_p(i) =
 6.87144*10^-8+4.7578*10^-10*T_prod(i)-1.4646*10^-12*T_prod(i)^2;
    a_f(i) =
 9.8777*10^-8-1.2569*10^-11*T_prod(i)-3.8286*10^-14*T_prod(i)^2;
    a_a(i) =
 1.2461*10^-7+3.7321*10^-10*T_prod(i)-1.2244*10^-12*T_prod(i)^2;
    a_w(i) =
 1.3168*10^-7+62477*10^-10*T_prod(i)-2.4022*10^-12*T_prod(i)^2;
    a_i(i) = 1.1756*10^-6 -60833*10^-9*T_prod(i) +
 9.5037*10^-11*T_prod(i)^2;

    a(i) = 1/(x_p/a_p(i) + x_f/a_f(i) + x_a/a_a(i) + x_w(i)/a_w(i) +
 x_ice(i)/a_i(i));

    %specific volume
    xV_w(i) = x_w(i)/rho_w(i)*mean_rho(i);
    xV_ice(i) = x_ice(i)/rho_ice(i)*mean_rho(i);
    xV_p(i) = x_p/rho_p(i)*mean_rho(i);
    xV_f(i) = x_f/rho_p(i)*mean_rho(i);
    xV_a(i) = x_a/rho_a(i)*mean_rho(i);


    k_ice_w(i) = k_ice(i)*((1-xV_w(i)^(2/3))/(1-xV_w(i)^(2/3)*(1-
xV_w(i)^(1/3))));
    k_ice_w_p(i) = k_ice_w(i)*((1-xV_p(i)^(2/3))/(1-xV_p(i)^(2/3)*(1-
xV_p(i)^(1/3))));
    k_ice_w_p_f(i) = k_ice_w_p(i)*((1-xV_f(i)^(2/3))/(1-
xV_f(i)^(2/3)*(1-xV_f(i)^(1/3))));
    k_ice_w_p_f_a(i) = k_ice_w_p_f(i)*((1-xV_a(i)^(2/3))/(1-
xV_a(i)^(2/3)*(1-xV_a(i)^(1/3))));

    %specific heat capacity
    cp(i) = 1.55+1.26*x_s+((x_wo-x_b)*L_0*T_int)/T_prod(i);

    %effusivity
    effu(i) = sqrt(k_ice_w_p_f_a(i)*cp(i)*mean_rho(i));

%     k_parallell(i) = k_w(i)*xV_w(i) + k_ice(i)*xV_ice(i) +
 k_p(i)*xV_p(i) + k_f(i)*xV_f(i) + k_a(i)*xV_a(i);
%     k_perpendicular(i) = 1/(xV_w(i)/k_w(i) + xV_ice(i)/k_ice(i) +
 xV_p(i)/k_p(i) + xV_f(i)/k_f(i) + xV_a(i)/k_a(i));
end

conductivity = k_ice_w_p_f_a;

diffusivity = conductivity./(cp.*mean_rho);

plot(T_prod,a);
```

```
grid on
xlabel('Temperature')
ylabel('Diffusivity')
title('Diffusivity as a function of Temperature')

ans = zeros(length(a), 2);

ans(:,1) = mean_rho;
ans(:,2) = a;
ans(:,3) = effu;


end
```

10.4.6 Function creating a logical assessment if the node is located on the surface

```
function ans = Surface(dx,dtheta,nr)


% Geometry descritization
Lx = -0.3:dx:0.7;
theta = -dtheta:dtheta:pi/2;


for i= 2:length(Lx)-1 %Runs through each cross section in x-direction
   for j = 1:length(theta)
        for  r = 1:nr
            %Nodes inside the fish
            mat(i,j,r) = false; % set default node is not on surface

            if r == nr %surface of fish
                mat(i,j,r) = true;
            end

            if i == 2 %first cross section
                mat(i,j,r) = true;
            end

            if i == length(Lx)-1 %last cross section
                mat(i,j,r) = true;
            end
        end %r
   end %theta
end %x

ans = mat;

end %function
```

```
Not enough input arguments.

Error in Surface (line 5)
Lx = -0.3:dx:0.7;
```

Published with MATLAB® R2017b

10.4.7 Plots the heat load as a function of time

```
function ans = effect_plot

%collects the heat load vectors calculated from tunaHeat
eff1
eff2
eff3

k = 1;%counter
for i = 0:length(eff3)
    if mod(i,10) == 1
        if i>1
        if i <= length(eff1)
        %Calculates the mean value for the last 10 heat load values
        newEff1(k) = mean(eff1(i-9:1:i));
        newEff2(k) = mean(eff2(i-9:1:i));
        newEff3(k) = mean(eff3(i-9:1:i));
        elseif i<= length(eff2)
        newEff2(k) = mean(eff2(i-9:1:i));
        newEff3(k) = mean(eff3(i-9:1:i));
        else
        newEff3(k) = mean(eff3(i-9:1:i));
        end
        k = k+1;
        end
    end
end

%skip the first two hours to visualize the difference
newEff1(1:int16(length(newEff1)/12)) = [];
newEff2(1:int16(length(newEff2)/24)) = [];
newEff3(1:int16(length(newEff3)/48)) = [];

time1 = linspace(2,24,length(newEff1));
time2 = linspace(2,48,length(newEff2));
time3 = linspace(2,96,length(newEff3));

plot(time1,newEff1)
hold on
plot(time2,newEff2)
hold on
plot(time3,newEff3)
grid on
xlabel('time (hours)')
ylabel('heat load (kW)')
title('heat load vs time for 3 different sized tuna fish')

legend({'1 meter tuna','2 meter tuna','3 meter tuna'})
svar = 5;%random
end
```

Christian Mellbye and Sondre Bekken

Utilizing LNG for low temperature freezing system for tuna

NTNU
Norwegian University of
Science and Technology